REVIEW

Is fractional-order chaos theory the new tool to model chaotic pandemics as Covid-19?

Manashita Borah · Antara Gayan · Jiv Siddhi Sharma · YangQuan Chen · Zhouchao Wei · Viet-Thanh Pham

Abstract The deadly outbreak of the second wave of Covid-19, especially in worst hit lower-middle-income countries like India, and the drastic rise of another growing epidemic of *Mucormycosis*, call for an efficient mathematical tool to model pandemics, analyse their course of outbreak and help in adopting quicker control strategies to converge to an infection-free equilibrium. This review paper on prominent pandemics reveals that their dispersion is chaotic in nature having long-range memory effects and features which the existing integer-order models fail to capture. This paper thus puts forward the use of fractional-order (FO) chaos theory that has memory capacity and hereditary properties, as a potential tool to model the pandemics with more accuracy and closeness to their real physical dynamics. We investigate eight FO models of Bombay plague, Cancer and Covid-19 pandemics through phase portraits, time series, Lyapunov exponents and bifurcation analysis. FO controllers (FOCs) on the concepts of fuzzy logic, adaptive sliding mode and active backstepping control are designed to stabilise chaos. Also, FOCs based on adaptive sliding mode and active backstepping synchronisation are designed to synchronise a chaotic epidemic with a non-chaotic one, to mitigate the unpredictability due to chaos during transmission. It is found that severity and complexity of the models increase as the memory fades, indicating that FO can be used as a crucial parameter to analyse the progression of a pandemic. To sum it up, this paper will help researchers to have an overview of using fractional calculus in modelling pandemics more precisely and also to approximate, choose, stabilise and synchronise the chaos control parameter that will eliminate the extreme sensitivity and irregularity of the models.

Keywords Chaos · Control · Fractional-order · Pandemic · Plague · Cancer · Covid-19

M. Borah (✉) · A. Gayan · J. S. Sharma
Department of Electrical Engineering, Tezpur University, Tezpur, Assam 784028, India
e-mail: manabor@tezu.ernet.in;
manashitaborah@gmail.com

Y. Chen
Mechatronics, Embedded Systems and Automation (MESA) Lab, University California Merced, Merced, USA

Z. Wei
School of Mathematics and Physics, China University of Geosciences, Wuhan 430074, China

V.-T. Pham
Nonlinear Systems and Applications, Faculty of Electrical and Electronics Engineering, Ton Duc Thang University, Ho Chi Minh City, Vietnam

1 Introduction

With the second wave of Covid-19 turning grim in third world, lower-middle-income countries like India,

where numbers of infected cases and deaths per day until 12 May 2021 are reaching record highs of 0.4 million and 4000, respectively [38]; it is the urgent requirement for an efficient mathematical tool to model and analyse epidemics and pandemics to predict their future course of outbreak and help develop rapid control strategies. To add to this is the spread of another growing epidemic of a rare fungal infection *Mucormycosis* or the 'Black fungus' typically infecting Covid-19 recovered patients as reflected by the exponential surge of 9000 cases reported in India by May 2021 [12, 16, 19]. Since interactions among the species in a pandemic have a greater complexity, it is difficult to solve their models that describe the disease analytically. Henceforth, formulating the model mathematically with a suitable tool that can imitate the disease more accurately helps in detecting its behavioural dynamics [58].

A chaotic propagation of a pandemic is characterised by extreme sensitivity to slight variation in initial conditions (ICs) of physical factors such as rise in the number of asymptomatic carriers, number of infected cases and small increase in the number of undetected cases.[82]. While studying a novel ongoing pandemic, chaos theory has been a powerful approach to define, model and analyse the exponentially propagating dynamics and extracting the underlying deterministic component by taking into account crucial factors as: variables relevant for the pandemic, equations that govern these variables, parameter values, constraints of the model and reformulation of the equations based on existing observations [53].

In order to determine whether the dissemination of a pandemic is chaotic, the following criteria may be taken into account [39]:

1. *Aperiodicity,* i.e. multiple solutions of the pandemic model exist, such that no two solutions repeat,
2. *Sensitive,* i.e. the epidemic is highly sensitive and give rise to divergent dynamics on a slight change of physical factors,
3. *Long-term unpredictability,* i.e. the propagation of the pandemic is unexpected and cannot be foreseen from one point to another,
4. *Determinism,* i.e. the outcome, amount and rate of spread, is determined by real changes in the physical conditions of the system.

Chaotic behaviour of pandemics have been extensively reported in low-mid-income countries such as, Plague epidemic in Bombay, India [51], chaotic epidemic crisis management in Mexico [72], Ebola Virus epidemic in Guinea, Liberia and Sierra Leone [52] and Dengue in Pakistan [4]; a brief review of this is given in the next section.

1.1 A brief review on impact of chaos on prominent epidemics

This section surveys some prominent epidemics that reveal chaotic dispersal.

1. Plague epidemic, India (1896–1911)

The Bombay epidemic, India, has been one of the earliest closely monitored diseases to have been recorded for investigating its causes, effect and control. The bubonic plague in 1896 did not stay confined to Bombay alone, it hit all over India [62]. The bacillus *Yersinia Pestis*, causing the bubonic plague, develops buboes in the infected, along with other symptoms such as fever, vomiting, bleeding and organ failure.

Impact of chaos (IOC): The earlier models of the bubonic plague [7] assume that a single species of rat and flea is responsible for the bubonic plague progression, and thus human infections are modelled as a by-product of rat infections. On the contrary, multiple epizootics of rats such as *Mus decumanus* and *Mus rattus* are reported to have caused the bubonic plague [61]. In 2015, a new model of plague, proposed in Mangiarotti [51] that took into account multiple epizootics of rats, led to the finding that the progression of the disease is chaotic in nature.

2. Spanish flu (1918–1920)

The Spanish flu is one of the first global pandemic reported to have occurred in the era of modern medicine where the nature and course of the disease were studied as it unfolded [35]. The H1N1 strain of the influenza virus activates a cytokine storm which damages the immune system. With a mortality rate of 20%, this pandemic is said to have killed more than 100 million people, hampering the economy during the World War I.

IOC: Though chaotic dynamics of the Spanish Flu is not extensively reported, however Upadhyay et al. [79]

reports that such influenza epidemics have bidirectional spread and are characterised by wave of chaos in a dominant mode.

3. HIV AIDS (1980–…)

The early eighties gave birth to a gradually growing pandemic of HIV/AIDS [35]. According to the recent WHO report, 76 million people have been infected with the HIV epidemic so far, 33 million have lost their lives and 38 million are presently infected by the end of 2019.

IOC: Bairagi et al. [8] reports that self-proliferation of host cells in non-delayed HIV models has chaotic immune response. Chaos is responsible for considerable fluctuations in host cells count in blood plasma of HIV patients.

4. Smallpox outbreak (1972)

The smallpox epidemic killed hundreds of millions of people up till the twentieth century with a mortality of 30%. Smallpox was eradicated in 1960s with mass vaccination on a global scale. However, the former Yugoslavia in 1972 saw a new wave of outbreak of smallpox. Though this outbreak was controlled within two months with mandatory revaccination, containment zones, quarantine measures, sealed borders and travel ban, yet it is significant for the research community to study the course of the outbreak as it marked the reappearance of an already eradicated epidemic.

IOC: Chaotic phenomenon has been reported to exist in smallpox epidemic models [29, 70]. Though smallpox is eradicated, however, its reappearance may be possible. As a result, Seward et al. [70] have devised an algorithm to supervise clinical and public health responses with respect to suspected smallpox cases.

5. Swine flu pandemic (April 2009–May 2010)

The Swine flu outbreak in Mexico in 2009, considered as a reprise of Spanish flu pandemic of 1918, rose steeply to pandemic proportions within weeks [77] infecting over 10% of the world population [26]. It was caused by H1N1 strain of the influenza virus.

IOC: The propagation of the epidemic in terms of chaotic waves is modelled in Upadhyay et al. [79], where conditions for Hopf and Turing bifurcations are evaluated. The reported models suggest that the Swine Flu epidemic has a complex dynamics of spatial spread through chaotic waves. Also the H1N1 flu strain can propagate both in forward and backward direction, i.e. the spread of influenza is bidirectional and that chaos phenomenon is an intrinsic property of dissemination of this epidemic.

6. Ebola virus epidemic (2013–2016)

The epidemic of the Ebola virus disease (EVD) appeared in Guinea, December 2013, from which it extended rapidly to Liberia and Sierra Leone and proved lethal until 2016. According to WHO database, the case fatalities rose till 90%. Ebola-Zaire, one of the five species of the Ebola virus, is responsible for infecting with a dangerous mortality rate of 70% [52].

IOC: The complex dynamical behaviour of the EVD epidemic, particularly in the middle stage of uncontrolled rapid propagation has been effectively defined by a chaotic model [52]. The chaotic model is derived from observational data released by WHO, and depicts that the diversified key parameters are difficult to be predicted and are dependent on the slightest change in ICs. This indicates that an uncontrolled case of chaos may result in an exponential rise in the number of infections and fatalities.

7. Cancer epidemic

As per WHO, cancer, one of the leading causes of death, is accounted for 9.6 million deaths in 2018 alone globally, with statistics of one in six deaths due to cancer. Cancer may be caused by chemical carcinogens such as drinking arsenic contaminated water and alcohol and smoking tobacco; physical carcinogens, such as being subjected to ultraviolet radiation; and biological carcinogens such as obesity, lack of physical activity or infections from viruses, bacteria etc. Recent literature reports studies on various forms of cancer epidemics, such as lung cancer epidemic [63], virus-related head and neck cancer epidemic [55] and liver cancer epidemic [23].

IOC: Itik and Banks [36] first reported the explicit existence of chaos in Cancer epidemic. Cancer models have been found to display deterministic chaos giving birth to complex oscillations indicative of long-term tumour relapse (Khajanchi et al., 2018) through period doubling route and Hopf bifurcations.

8. Dengue epidemic

WHO reports severe dengue epidemics re-emerged in 1950s in the South Asian countries of Philippines and Thailand with a comparatively recent outbreak in Singapore, 2005 [59]. Dengue is a mosquito-borne viral epidemic infecting 3.9 billion people in 128 countries, killing more than 20,000 people in 2012 [18].

IOC: Chaos results in high seasonality and complexity in the Dengue models [56]. This explains the irregular fluctuations in the empiric outbreak data of the Dengue epidemic [2]. Also, it is discovered that temporary cross-immunity expands the parameter range of chaotic dynamics leading to coexisting attractors [2] eventually causing multiple routes to chaos in Dengue epidemic models.

9. Cholera epidemic

The epidemic of Cholera first appeared in India in 1817 [24] and later spread to 52 countries infecting 4.3 million people worldwide. Cholera quickly spreads in densely populated areas with poor water sanitation. The prime symptoms of infection are severe watery diarrhoea, vomiting, body ache, fall in blood pressure, kidney failure, and if untreated may lead to death within 24 h [73].

IOC: Righetto et al. [68] have reported that the spread of cholera is chaotic with increasing values of the degree of seasonality. Parameter estimation and sensitivity analysis reveal the deterministic behaviour of the Cholera epidemic model [10].

10. Covid-19 pandemic

The most lethal of pandemics recently known with a deadly rate of exponential dissemination is the Coronavirus disease that broke out in 2019 (Covid-19). Jones and Strigul [39] considered global data set from 22 January to 30 May 2020, corresponding to 267 countries and have suggested that COVID-19 manifests the major qualitative characteristics of a chaotic system.

IOC: The vital factors for modelling Covid-19 pandemic such as number of confirmed cases per day, number of critical cases under intensive care per day and the cumulated number of fatalities per day have been found to interact chaotically [53]. The fractal dimension and the phase portrait analyses carried out

in [31] reveal that Covid-19 is chaotic in nature. In fact, application of chaos theory to model Covid-19 is reported to be a promising tool in decision-making, thereby helping in tracking the effectiveness of control measures especially in countries where the number of cases are relatively low and rapid enforcement of control measures need to be adopted to prevent a catastrophic evolution of the pandemic [39].

1.2 Fractional-order (FO) dynamics of chaotic epidemic models

The literature survey carried out in previous section indicates that the modelling of epidemics is confined to IO models (IOMs) which often fail to encompass in-depth understanding of the dynamics of the epidemic such as contribution of asymptomatic transmission, range of unpredictability, critical cases with comorbidities and effect of past history of data. [41]. These limitations can be overcome by incorporating the extraordinary advantages of FO models (FOMs) in modelling real physical phenomena and improving control performance. The differences between FOM and IOM are as follows:

1. FO derivative being a non-ideal operator can incorporate non-ideal, i.e. non-integer values along with integer values, unlike models governed by IO derivatives which can incorporate only ideal, i.e. IO values.
2. FO derivative being a non-local operator has the capacity to store infinite memory of the past values calculated until the present time, unlike IO derivative which is a memory-less operator.
3. The FO parameter of FO derivatives is an additional parameter that grants the control engineers flexibility to incorporate more constraints for an efficient design.
4. The FO controllers have a larger stability region [25] and robustness [50] against plant uncertainties compared with IO controllers.

The solutions to the diffusion equation with fractional-order propagation are obtained at a quicker rate than the ordinary diffusion equation and may be asymmetric [30]. The FO chaotic epilepsy model proposed by Tene et al. [76] reported that the FOM induces faster synchronisation than IOM. Jan et al. [37], proposed the FOM of Dengue epidemic and found that the additional properties of heredity and

memory effects of fractional calculus provide more realistic information about Dengue transmission through asymptomatic carriers. Recently, FOMs of Diabetes, HIV, Dengue, Migraine, Parkinson's and Ebola Virus diseases proposed in Borah et al. [12, 16] revealed inherent unobserved dynamics as the FO varies. FOMs have lesser error compared to IOMs while delivering a closer fit to real data [65, 66]. As the propagation of COVID-19 is chaotic with long-range memory, it is essential to use a memory-enabled tool to model it. We blend the superior merits of fractional calculus with chaos theory [13, 14] to derive an adequate mathematical model, which behaves as close as possible to the practical epidemic.

1.3 Control of chaos in mathematical models of epidemics

This section presents a brief review on existing control strategies to stabilise and synchronise chaos in the mathematical models of epidemics as given in Table 1.

A state-dependent impulsive feedback controller is proposed [64] to regulate the spread of infectious epidemics like SARS, Dengue and Zika virus. Zhang et al. [86] have reported that an epidemic converges to a disease-free periodic solution if its threshold dynamics is controlled via reproduction number R_o. He and Banerjee [33] proposes a hard limiter controller to mitigate the dissemination of common influenza and H1N1 influenza epidemic. Seasonal outbreak of these types of infectious diseases is a natural phenomenon, so it is important to study epidemic models with seasonal fluctuation [85]. The hard limiter controller is applied to an epidemic model with seasonality and external noise, and it was found that variation in parameters such as temporary immunity rate, seasonality degree, noise degree and fractional order induce high sensitivity resulting in a chaotic model. For smaller values of the limiter, the system tends to a periodic system or a stable system, i.e. the disease tends to vanish. The dissipative control strategy [22] for a susceptible, infected and recovered (SIR)-type descriptor epidemic system like HBV (Hepatitis B virus) with nonlinear incidence rates bound by fuzzy characteristics is designed to control the change in the birth rate of population in the epidemic model to suppress chaos. A robust H_∞

controller [21] is designed for discrete SI-type epidemic model with nonlinear incidence rates where the intrinsic birth rate is varied so that chaotic responses of the states of susceptible and infected in the epidemic disappear. A tracking controller [84] is designed such that the percentage of infective disease converges to zero to stabilise chaos in the epidemic model. Similarly, the tracking controller for stabilising hyperchaos in SEIR-type epidemic system with nonlinear transmission rate is designed in Yi et al. [83]. Active control method is proposed in Ansari et al. [6] such that the error states which are functions of susceptible, infected and information variables converge to zero [40] and thereby synchronisation is accomplished. Tan et al., [74] and Zhang et al. [85] propose a feedback control technique applied to SIR-type epidemic model with seasonal fluctuations for H1N1 and common influenza where Neimark-Sacker bifurcation period doubling route to chaos is discovered.

Some other control strategies such as optimal control based on two time-dependent control variables, viz insecticide use and vaccination [10] and predictive control strategy to determine the time and duration of social distancing policies [32], have been applied to Cholera epidemic, Dengue epidemic [4] and Covid-19 pandemic, respectively. However, they are all confined to IOMs only.

This paper aims to bridge the research gap between:

1. application of FO chaos theory to model pandemic propagation dynamics (chaotic and non-chaotic) that are not captured by IOMs,
2. application of FO strategies in controlling and synchronising these chaotic epidemic models to a disease-free equilibrium.

2 Fundamentals of FO calculus for modelling and control

The modelling of the epidemics and design of controllers to attain synchronisation is determined by FO stability theorems whose preliminaries are presented below.

The Caputo fractional derivative of order α of a continuous function $f(t)$ is defined as in (1).

Table 1 Recent survey of control methods applied to epidemics modelled using chaos theory

Sl. no	Works	Year	Control method	Chaotic epidemic model	Fractional order
1	Borah et al	2021	Backstepping, Adaptive Feedback, SMC	Diabetes, HIV, Dengue, Migraine, Parkinson's and Ebola Virus diseases	Yes
2	Mangiarotti et al	2020	No	COVID-19	No
3	Rihan et al	2019	No	SIR (Ebola Virus, Dengue, Influenza A, HIV)	Yes
4	Li et al	2019	State-dependent feedback control	SIR (SARS, Dengue fever, Zika Virus)	No
5	Duarte et al	2019	No	SIR (Avian Influenza)	No
6	He et al	2018	Hard Limiter Control	SIR (common influenza and H1N1 influenza outbreak)	Yes
7	Abdelaziz et al	2018	No	Discrete SI (Avian influenza)	Yes
8	Chang et al	2018	Dissipative control	SIR (Hepatitis B Virus)	No
9	Chang et al	2017	Robust H-infinity control	SI (SARS, MERS, Ebola, HIV, Hepatitis)	No
10	Upadhyay et al	2016	No	SEIR Ebola virus	No
11	Mangiarotti et al	2016	No	Ebola virus	No
12	Tan et al	2015	Feedback control method	Discrete SI (SARS, MERS, Ebola)	No
13	Magiarotti	2015	No	Plague (1896–1911)	No
14	Ansari et al	2014	Active control method	SIR (Avian Human influenza, measles)	Yes
15	Upadhyay et al	2014	No	SI (Influenza virus)	No
16	Hu et al	2014	No	Discrete SIR epidemic model (HIV, measles, SARS)	No
17	Pedro et al	2014	No	Rift Valley Fever epidemic model	No
18	Zhang et al	2013	Feedback controller	SIR epidemic model (common influenza and H1N1 influenza)	No
19	Kooi et al	2013	No	Multi-strain epidemiology model (Dengue fever)	No
20	Yi et al	2011	Tracking controller	Discrete SI epidemic model (Hepatitis B and C, HIV)	No
21	Li et al	2010	No	SI (SARS, influenza)	No
22	Yi et al	2009	Tracking controller	SEIR (measles and SARS)	No
23	Ahmed et al	2007	No	Foot and Mouth disease, SARS and Avian flu	Yes

$$D_t^\alpha f(t) = \frac{\mathrm{d}^\alpha f(t)}{\mathrm{d}t^\alpha} = \begin{cases} \dfrac{1}{\Gamma(w-\alpha)} \displaystyle\int_0^t \dfrac{f^{(w)}(\tau)}{(t-\tau)^{\alpha-w+1}}\,\mathrm{d}\tau, & w-1 < \alpha < w, \quad w \in N \\ \dfrac{\mathrm{d}^w}{\mathrm{d}t^w} f(t), & \alpha = w \end{cases} \tag{1}$$

Let us define an FO nonlinear system (FONLS) as in (2),

$$D_t^\alpha x(t) = f(x(t), t) \qquad (2)$$

where the FOs lie in $0 < \alpha < 1$ and $x(t) = [x_1, x_2, \ldots, x_n]^T, f(x(t), t) = [f_1(x(t)), f_2(x(t)), \ldots, f_n(x(t))]^T$ $(i = 1, 2, \ldots, n)$.

Theorem 1 ([20]). *The equilibrium points of a commensurate FONLS are asymptotically stable if for all the eigenvalues $\lambda_i, (i = 1, 2, \ldots, n)$ of the Jacobian matrix $J = \partial f / \partial x$, where $f = [f_1, f_2, \ldots, f_n]^T$, evaluated at the equilibrium point, satisfy the condition: $|\arg(\mathrm{eig}(J))| = |\arg(\lambda_i)| \rangle \alpha \pi / 2, i = 1, 2, \ldots, n$.*

Lemma 1 ([3, 15]). *If $x(t) \in \mathbb{R}$ is a continuous and derivable function, then, for any time instant ≥ 0,*

$$\frac{1}{2} D^\alpha x^2(t) \leq x(t) D^\alpha x(t), \quad \forall \alpha \in (0, 1]$$

where $D^\alpha x(t)$ is the Caputo fractional derivative of $x(t)$ of FO α.

2.1 Computation of the fractional-order differential equations (FODEs)

The Adams–Bashforth–Moulton method established on the predictor–corrector technique [27] is used to solve the FODEs. The FONLS (2) may be written in a Volterra integral equation as in (3),

$$x_i(t) = x_i(0) + \frac{1}{\Gamma \alpha} \int_0^t (t - \tau)^{\alpha - 1} f_i(x_1, x_2, \ldots, x_n) \mathrm{d}\tau \qquad (3)$$

where $x_i(0)$ are ICs of $x_i(t)$.

The corrector equation obtained by substituting $h = \frac{T}{N}, t_n = nh$, for $(n = 0, 1, \ldots, N)$ for a unique solution in $[0, T]$ is as in (4).

$$x_{ih}(t_{n+1}) = x_i(0) + \frac{h^\alpha}{\Gamma(\alpha + 2)}$$
$$f_i\left(x_{1h}^p(t_{n+1}), x_{2h}^p(t_{n+1}), \ldots, x_{nh}^p(t_{n+1})\right)$$
$$+ \frac{h^\alpha}{\Gamma(\alpha + 2)} \sum a_{i,j,n+1} f_i\left(x_1(t_j), x_2(t_j), \ldots, x_n(t_j)\right) \qquad (4)$$

where $a_{i,j,n+1} = \begin{cases} n^{\alpha+1} - (n - \alpha)(n+1)^\alpha, \text{if } j = 0 \\ (n-j+2)^{\alpha+1} + (n-j)^{\alpha+1} - 2(n-j+1)^{\alpha+1}, \text{if } 1 \leq j \leq n \\ 1, \text{if } j = n+1 \end{cases}$

The predicted value $x_{ih}^p(t_{n+1})$ is determined by (5),

$$x_{ih}^p(t_{n+1}) = x_i(0) + \frac{1}{\Gamma(\alpha)} \sum_{j=0}^n b_{i,j,n+1} f_i\left(x_{ih}(t_j)\right) \qquad (5)$$

where $b_{i,j,n+1} = \frac{h^\alpha}{\alpha}((n - j + 1)^\alpha - (n - j)^\alpha), 0 \leq j \leq n$.

Errors are estimated by (6),

$$e = \max\left\{\max|x_1(t_j) - x_{1h}(t_j)|, \max|x_2(t_j) - x_{2h}(t_j)|, \ldots, \max|x_n(t_j) - x_{nh}(t_j)|\right\} = O(h^\rho) \qquad (6)$$

where $j = (0, 1, 2, \ldots, N), \rho = \min\{2, 1 + \alpha\}$.

These theorems and definitions will be used in the proposed models and controllers designed in Sect. 5.

3 Proposed FO epidemic models (FOEMs) and design of FO controllers

This section presents FO chaotic models of three pandemics: Plague, Cancer and Covid-19, and design of FO control strategies to stabilise and synchronise chaos in the models.

3.1 FO Plague epidemic models (FOPEMs)

IOMs of chaotic plague epidemic models were proposed in Mangiarotti [51]. We present six FOPEMs, where x_1, x_2 and x_3 represent the numbers of human plague deaths, captured infected rats of the *M. decumanus* species and captured infected rats of the *M. rattus* species, respectively [12, 16].

(a) FOPEM M_0
M_0 is a 10-term chaotic model given as in (7), where the tuning parameter $\vartheta = 0.598$.

$$\begin{cases} D^\alpha x_1 = -0.0976 x_3^2 + 0.045 x_2 x_3 - 12.6237 \vartheta x_1 \\ D^\alpha x_2 = 0.0107 x_2^2 - 0.0237 x_1 x_2 \\ D^\alpha x_3 = 0.0108 x_3^2 + 1.4512 x_2 - 5.912 x_1 - 0.0147 x_1 x_3 \\ \qquad\qquad + 0.0041 x_1 x_2 \end{cases} \qquad (7)$$

(b) FOPEM M_1
M_1 is a 11-term chaotic model given as in (8), where $\vartheta = 1$.

$$\begin{cases} D^{\alpha}x_1 = -0.0976x_3^2 + 0.045x_2x_3 - 12.6237\vartheta x_1 \\ D^{\alpha}x_2 = 0.0107x_2^2 - 0.0237x_1x_2 \\ D^{\alpha}x_3 = 0.0213x_3^2 + 2.0814x_2 - 6.917x_1 - 0.0255x_1x_3 \\ \qquad\qquad +0.0078x_1x_2 - 0.0013x_2^2 \end{cases} \tag{8}$$

(c) FOPEM M_2

M_2 is also a 11-term chaotic model given as in (9), where $\vartheta = 0.9$.

$$\begin{cases} D^{\alpha}x_1 = -0.1434x_3^2 + 0.0674x_2x_3 - 12.7264\vartheta x_1 \\ \qquad\qquad -0.0025x_2^2 \\ D^{\alpha}x_2 = 0.0107x_2^2 - 0.0237x_1x_2 \\ D^{\alpha}x_3 = 0.0108x_3^2 + 1.4512x_2 - 5.912x_1 \\ \qquad\qquad -0.0147x_1x_3 + 0.0041x_1x_2 \end{cases} \tag{9}$$

(d) FOPEM M_3

M_3 is a 12-term chaotic model given as in (10), where $\vartheta = 0.945$.

$$\begin{cases} D^{\alpha}x_1 = -0.0936x_3^2 + 0.0431x_2x_3 - 12.0677\vartheta x_1 \\ D^{\alpha}x_2 = 0.0103x_2^2 - 0.0227x_1x_2 (10) \\ D^{\alpha}x_3 = 0.0318x_3^2 + 1.7263x_2 - 6.6007x_1 \\ \qquad\qquad -0.0355x_1x_3 + 0.005967x_1x_2 - \\ \qquad\qquad 0.004x_1^2 - 0.00007x_2^2 \end{cases} \tag{10}$$

(e) FOPEM M_4

M_4 is a 10-term periodic model given as in (11), where $\vartheta = 1$.

$$\begin{cases} D^{\alpha}x_1 = -0.0976x_3^2 + 0.045x_2x_3 - 12.6237\vartheta x_1 \\ D^{\alpha}x_2 = 0.0107x_2^2 - 0.0237x_1x_2 \\ D^{\alpha}x_3 = 0.0108x_3^2 + 1.4512x_2 - 5.912x_1 \\ \qquad\qquad -0.0147x_1x_3 + 0.0041x_1x_2 \end{cases} \tag{11}$$

(f) FOPEM M_5

M_5 is a 11-term periodic model given as in (12), where $\vartheta = 1$

$$\begin{cases} D^{\alpha}x_1 = -0.1434x_3^2 + 0.0674x_2x_3 \\ \qquad\qquad -12.7264\vartheta x_1 - 0.0025x_2^2 \\ D^{\alpha}x_2 = 0.0107x_2^2 - 0.0237x_1x_2 \\ D^{\alpha}x_3 = 0.0108x_3^2 + 1.4512x_2 - 5.912x_1 \\ \qquad\qquad -0.0147x_1x_3 + 0.0041x_1x_2 \end{cases} \tag{12}$$

Table 2 lists the dynamical analyses of FOPEMs to help predict critical transitions in biological systems [12, 16, 57].

Figure 1 depicts the attractors of the FOPEMs where M_0, M_1, M_2, M_3 are chaotic and M_4, M_5 are

periodic. A representative bifurcation diagram is plotted for the FOPEM M_3 at $\alpha = 0.995$ against the tuning parameter ϑ as the bifurcation parameter in Fig. 1g. The gradual evolution of chaos is distinctly visible through a period doubling pathway. The ranges of the tuning parameter for the corresponding attractor dynamics are $[0, 0.265]$: (period 1), $[0.265, 0.576]$: (period 2), $[0.576, 0.874]$: (period 4) and $[0.875, 1]$: (chaos). The value of ϑ is chosen as 0.945 for M_3 for chaotic dispersal. Similarly, ϑ for other FOPEMs are chosen.

3.1.1 FO controllers (FOCs) for stabilisation of chaos in FOPEMs

Three stabilisation controllers are designed in three subsections dedicated to FO fuzzy logic control (FOFLC), FO adaptive sliding mode control (FOASMC) and FO active backstepping control (FOABC). It is to be noted that these controllers are applied to stabilise chaos only in those FOPEMs which have chaotic dynamics, i.e. M_0, M_1, M_2 and M_3 as discussed in Table 2.

3.1.1.1 FOFLC: The design of an IO-based TS fuzzy logic control (TSFLC) is reported in Vaidyanathan [80]. The configuration of the system with a fuzzifier which converts the crisp inputs to linguistic variables using the membership functions stored in the database, the inference engine which simulates decisions by performing approximate reasoning, and the defuzzifier which converts the fuzzy output values into crisp values is represented in the block diagram of Fig. 2.

Let a chaotic, nonlinear system be defined as in (2) and controlled system as in (13).

$$D^{\alpha}x(t) = f(x(t), t) + B.u \tag{13}$$

Here, $u = (u_1, u_2, \ldots, u_n)^{\mathrm{T}}$ is the control signal. The control input u in (13) is defined as in (14),

$$u_i = u_{eqi} + u_{Li} \tag{14}$$

where $i = 1, 2, 3, \ldots, n$, and $u_{eq} = m(x_1, x_2, x_3, \ldots, x_n)$ is an n-dimensional vector field containing continuous, nonlinear functions. In FOFLC, u is calculated by weighted sum defuzzification method, and B is an $n \times n$ identity matrix. Let X be the universe of discourse for the system defined in (13) and u_L be based on fuzzy control rules.

Table 2 Investigation of dynamics of the FO Plague epidemic models

Model	ICs	Equilibrium points	Eigen values $(\lambda_i, i = 1, 2, 3)$	FO	Bounds of ϑ	LEs	Dynamics
M_0	(166.8903, 1070.193, 138.7208)	$E_1 = (- 2723.906, 0, - 459.002)$ $E_2 = (0,0,0)$ $E_3 = (428.4239, 948.939, 97.436)$	$\lambda_{1,2,3} = (64.556, - 9.44, 32.0185)$ $\lambda_{1,2,3} = (- 7.5489, 0, 0)$ $\lambda_{1,2,3} = (- 7.2477, 2.8296 + 11.2178\,i, 2.8296 - 11.2178\,i)$	0.98	[0.375, 0.75]	$LE_1 = 0.059548$ $LE_2 = 0$ $LE_3 = - 3.0896$	Chaotic
M_1	(895.9957, 2391.688, 312.7087)	$E_1 = (0,0,0)$ $E_2 = (- 1112.367, 0, - 379.308)$ $E_3 = (533.355, 1181.3568, 200.333)$	$\lambda_{1,2,3} = (- 12.623, 0, 0)$ $\lambda_{1,2,3} = (26.363, - 19.1324, 18.7156)$ $\lambda_{1,2,3} = (- 7.8815, 1.4159 + 12.3523\,i, 1.4159 - 12.3523\,i)$	0.98	[0.57, 1]	$LE_1 = 0.22158$ $LE_2 = 0$ $LE_3 = - 0.45977$	Chaotic
M_2	(836.9658, 1721.620, 328.9299)	$E_1 = (0,0,0)$ $E_2 = (- 2659.1148, 0, - 460.8589)$ $E_3 = (512.1487, 1134.3856, 178.6772)$	$\lambda_{1,2,3} = (- 11.453, 0, 0)$ $\lambda_{1,2,3} = (63.0210, - 14.0915, 31.7721)$ $\lambda_{1,2,3} = (- 7.9728, 2.4939 + 12.7008\,i, 2.4939 - 12.7008\,i)$	0.995	[0.83, 0.92]	$LE_1 = 0.32517$ $LE_2 = 0$ $LE_3 = - 6.099$	Chaotic
M_3	(344.0896, 627.7882, 101.5058)	$E_1 = (810.5939, 1786.4544, 145.9542)$ $E_2 = (1125.8296, 2481.1972, 1006.1933)$ $E_3 = (0,0,0)$	$\lambda_{1,2,3} = (- 17.624, 2.5635 + 19.2493\,i, 2.5635 - 19.2493\,i)$ $\lambda_{1,2,3} = (- 6.9833 + 14.039\,i, - 6.9833 - 14.039\,i, 52.146)$ $\lambda_{1,2,3} = (- 11.403, 0, 0)$	0.995	[0.875, 1]	$LE_1 = 0.76966$ $LE_2 = 0$ $LE_3 = - 15.0367$	Chaotic
M_4	(166.8903, 1070.193, 138.7208)	$E_1 = (0,0,0)$ $E_2 = (- 1911.3082, 0, - 497.203)$ $E_3 = (532.1154, 1178.6108, 200.9904)$	$\lambda_{1,2,3} = (- 12.623, 0, 0)$ $\lambda_{1,2,3} = (45.298, - 16.6145, 21.3474)$ $\lambda_{1,2,3} = (- 6.1764, 1.3416 + 12.8042\,i, 1.3416 - 12.8042\,i)$	0.937	[0.75, 1]	$LE_1 = 0$ $LE_2 = - 0.33791$ $LE_3 = - 6.4779$	Periodic
M_5	(836.9658, 1721.620, 328.9299)	$E_1 = (0,0,0)$ $E_2 = (534.5436, 1183.9892, 203.8006)$ $E_3 = (654.4082, 1449.4837, 486.6842)$	$\lambda_{1,2,3} = (- 12.726, 0, 0)$ $\lambda_{1,2,3} = (- 7.4083, 1.9474 + 13.0348\,i, 1.9474 - 13.0348\,i)$ $\lambda_{1,2,3} = (4.9346, - 0.6295 + 19.7595\,i, - 0.6295 - 19.7595\,i)$	0.96	[0.92, 1]	$LE_1 = 0$ $LE_2 = - 0.059592$ $LE_3 = - 6.4876$	Periodic

The ith fuzzy control rule base for the FOFLC is defined as in (15),

Rule: IF x_1 is $X_{i,1}$ AND...AND x_n is $X_{i,n}$,THEN u_L
$= u_i(x), i = 1, \ldots, r, \ r \in N$

$$\text{(15)}$$

where $X_{i,1}, X_{i,2}, \ldots, X_{i,n}$ are fuzzy sets describing the linguistic terms (LTs) of input variables, $u_L = u_i(x)$ is the control input of rule i and r is the total number of fuzzy rules.

Each fuzzy rule defined in (15) generates a weight defined as in (16).

$$\omega_i \in [0,1], i = 1, \ldots, r \tag{16}$$

From (16), it is assumed that for any $x \in X$ in the input universe of discourse X, there exists at least one weighted output among all rules that is nonzero. FO Lyapunov stability theorem applied to control the epidemic to a disease free equilibrium is as follows.

Theorem 2: ([47]). *Let the origin be an equilibrium of the controlled epidemic* (13), *and there exists a Lyapunov function,* $V(x) = x^T T x$, *where T is a positive definite matrix, on domain X containing the origin of R^n such that $D^\alpha V(x) \leq 0$, for $x \in X$. Let $S = \{x \in X : D^\alpha V(x) = 0\}$. If except the trivial solution $x(t) \equiv 0$, there is no solution of* (13) *that exists identically in S; then, the infection-free equilibrium at the origin is asymptotically stable in the domain X.*

On adding FOFLC to the FOPEM M_0 (7), we get (17).

$$\begin{cases} D^\alpha x_1 = -0.0976x_3^2 + 0.045x_2x_3 - 12.6237\vartheta x_1 + u_1 \\ D^\alpha x_2 = 0.0107x_2^2 - 0.0237x_1x_2 + u_2 \\ D^\alpha x_3 = 0.0108x_3^2 + 1.4512x_2 - 5.912x_1 \\ \qquad\qquad -0.0147x_1x_3 + 0.0041x_1x_2 + u_3 \end{cases}$$

$$\text{(17)}$$

On comparing (17) with (13), we have,

$f(x_1, x_2, x_3)$

$$= \begin{bmatrix} -0.0976x_3^2 + 0.045x_2x_3 - 7.5489726x_1 \\ 0.0107x_2^2 - 0.0237x_1x_2 \\ 0.0108x_3^2 + 1.4512x_2 - 5.912x_1 - 0.0147x_1x_3 \\ +0.0041x_1x_2 \end{bmatrix}$$

$$\text{and } B.u = \begin{bmatrix} 1 & 0 & 0 \\ 0 & 1 & 0 \\ 0 & 0 & 1 \end{bmatrix} \cdot \begin{bmatrix} u_1 \\ u_2 \\ u_3 \end{bmatrix} \tag{18}$$

u_{eq1}, u_{eq2} and u_{eq3} of (14) are selected as in (19).

$$\begin{cases} u_{eq1} = 0.0976x_3^2 - 0.045x_2x_3 \\ u_{eq2} = -0.0107x_2^2 + 0.0237x_1x_2 \\ u_{eq3} = -0.0108x_3^2 + 0.0147x_1x_3 - 0.0041x_1x_2 \end{cases}$$

$$\text{(19)}$$

Replacing (19) in (17) and (18), we get (20).

$$\begin{cases} D^\alpha x_1 = -7.5489726x_1 + u_{L1} \\ D^\alpha x_2 = u_{L2} \\ D^\alpha x_3 = 1.4512x_2 - 5.912x_1 + u_{L3} \end{cases} \tag{20}$$

The fuzzification module of FOFLC in Fig. 3 shows the triangular membership function of the LTs of the chosen linguistic variable x_1. Notations P, Z and N represent 'positive','zero' and 'negative', respectively, and the parameters chosen are $b3 = 200$, $b2 = 190$, $b1 = 10$, $a1 = 10$, $a2 = 1590$ and $a3 = 1600$.

Table 3 describes the set of fuzzy control rules.

The universe of discourse is, $X = [-200, 1600] \times [0, 2500] \times [-200, 400]$.

The Lyapunov function is chosen as (21).

$$V(x) = \frac{1}{2}\left(x_1^2 + x_2^2 + x_3^2\right) \tag{21}$$

Using Lemma 1,

$$D^\alpha V(x) \leq x_1 u_{L1} - 7.5489726x_1^2 + x_2 u_{L2} \\ + 1.4512x_2x_3 - 5.912x_1x_3 + x_3 u_{L3} \tag{22}$$

Using Theorem 2, $D^\alpha V(x) = 0 \iff x = [0,0,0]^T$ which implies $S = \{0,0,0\}$. Since Theorem 2 is satisfied in the FO sense, the designed FOFLC converges the controlled epidemic M_0 to an infection-free asymptotically stable equilibrium. Similarly, the FOFLCs for the chaotic FOPEMs $M_k, k = 0, ..., 3$, and fuzzy rules R_i $i = 1, 2, 3$ are designed as given in Table 4.

3.1.1.2 FOASMC: The function $f(x(t), t) = [f_1(x), f_2(x), \ldots, f_n(x)]^T$ in FONLS (2) is an n-dimensional vector field which can be further broken into smooth functions as in (23),
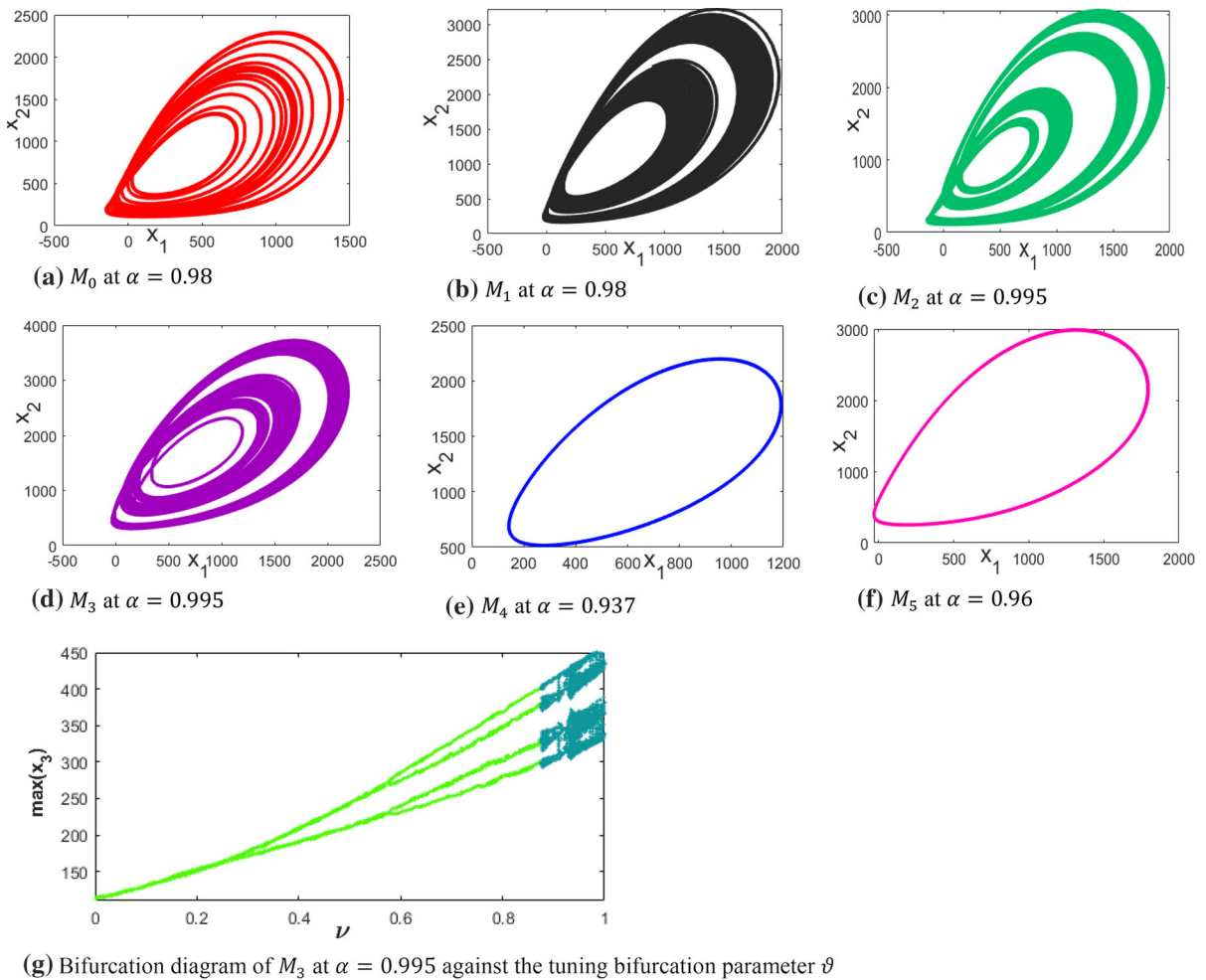
(a) M_0 at $\alpha = 0.98$

(b) M_1 at $\alpha = 0.98$

(c) M_2 at $\alpha = 0.995$

(d) M_3 at $\alpha = 0.995$

(e) M_4 at $\alpha = 0.937$

(f) M_5 at $\alpha = 0.96$

(g) Bifurcation diagram of M_3 at $\alpha = 0.995$ against the tuning bifurcation parameter ϑ

Fig. 1 Dynamical analysis of the FO Plague epidemic models

$$
\begin{cases}
D^\alpha x_1 = a(x_1, x_2, x_3, \ldots, x_n) - \varphi x_1 \\
D^\alpha x_2 = x_1.b(x_1, x_2, x_3, \ldots, x_n) + x_3.d(x_1, x_2, x_3, \ldots, x_n) - \beta x_2 \\
D^\alpha x_3 = x_1.c(x_1, x_2, x_3, \ldots, x_n) - x_2.d(x_1, x_2, x_3, \ldots, x_n) - \gamma x_3 \\
\qquad\qquad\qquad \vdots \\
\qquad\qquad\qquad \vdots \\
D^\alpha x_n = x_1.e(x_1, x_2, x_3, \ldots, x_n) - x_{n-1}.g(x_1, x_2, x_3, \ldots, x_n) \\
\qquad - \ldots - \tau x_n
\end{cases}
\tag{23}
$$

where $a(\bullet), b(\bullet), c(\bullet), d(\bullet), e(\bullet), \ldots, g(\bullet)$ are smooth functions belonging to $R^n \to R$ space and $\varphi, \beta, \gamma, \ldots, \tau$ are positive constants [69].

An adaptive switching surface $s(t)$ is considered such that the system satisfies the following condition in (24) to operate in sliding mode.

$$
s(t) = x_1(t) + \theta(t) = 0 \tag{24}
$$

$\theta(t)$ is an adaptive function whose fractional derivative is given in (25),
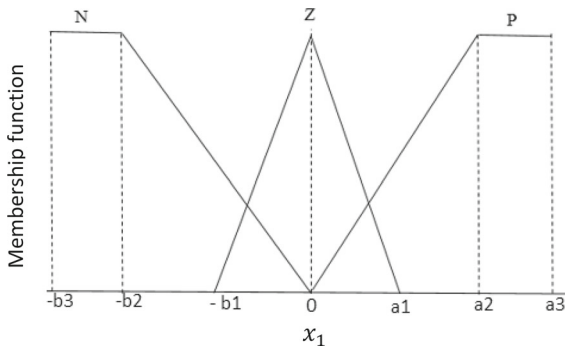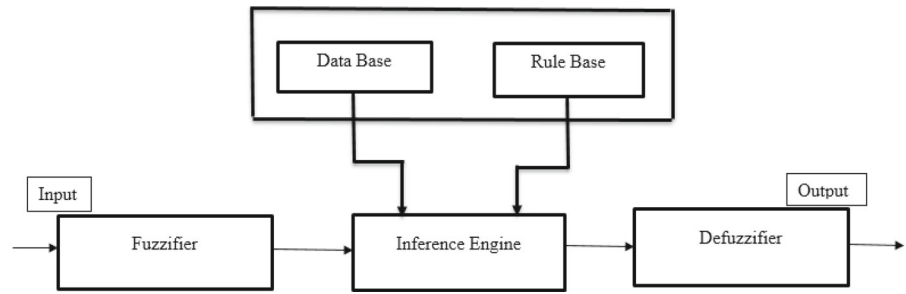
Fig. 2 Fuzzy logic control system

Fig. 3 Membership function for FOFLC

$$D^{\alpha}\theta(t) = x_2.b(x_1, x_2, x_3, \ldots, x_n) \\ + x_3.c(x_1, x_2, x_3, \ldots, x_n) + \ldots \\ + x_n.e(x_1, x_2, x_3, \ldots, x_n) + \varphi x_1 + \rho x_1 \tag{25}$$

where ρ is an arbitrary positive constant.

Using Caputo fractional derivative in (24), we obtain (26).

$$D^{\alpha}x_1(t) = -x_2.b(x_1, x_2, x_3, \ldots, x_n) \\ - x_3.c(x_1, x_2, x_3, \ldots, x_n) - \ldots \\ - x_n.e(x_1, x_2, x_3, \ldots, x_n) - \varphi x_1 - \rho x_1 \tag{26}$$

Replacing the value of $D^{\alpha}x_1(t)$ from (26) into (23) yields (27).

$$\begin{cases} D^{\alpha}x_1 = -x_2.b(x_1, x_2, x_3, \ldots, x_n) - x_3.c(x_1, x_2, x_3, \ldots, x_n) - \ldots - x_n.e(x_1, x_2, x_3, \ldots, x_n) - \varphi x_1 - \rho x_1 \\ D^{\alpha}x_2 = x_1.b(x_1, x_2, x_3, \ldots, x_n) + x_3.d(x_1, x_2, x_3, \ldots, x_n) - \beta x_2 \\ D^{\alpha}x_3 = x_1.c(x_1, x_2, x_3, \ldots, x_n) - x_2.d(x_1, x_2, x_3, \ldots, x_n) - \gamma x_3 \\ \qquad\qquad\qquad . \\ \qquad\qquad\qquad . \\ \qquad\qquad\qquad . \\ D^{\alpha}x_n = x_1.e(x_1, x_2, x_3, \ldots, x_n) - x_{n-1}.g(x_1, x_2, x_3, \ldots, x_n) - \ldots - \tau x_n \end{cases} \tag{27}$$

Table 3 Fuzzy rule base of FOFLCs for FOPEM M_0

Fuzzy rule	Antecedent x_1	Consequent U_L	$D^{\alpha}V(x)$	Stability
1	P	$U_{L1} = \begin{bmatrix} 5.912x_3 \\ -x_2 - 1.4512x_3 \\ -x_3 \end{bmatrix}$	$-7.5489726x_1^2 - x_2^2 - x_3^2 < 0$	Stable in FO sense
2	N	$U_{L2} = \begin{bmatrix} 5.912x_3 \\ -8.5x_2 - 1.4512x_3 \\ -x_3 \end{bmatrix}$	$-7.5489726x_1^2 - 8.5x_2^2 - x_3^2 < 0$	
3	Z	$U_{L3} = \begin{bmatrix} 5.912x_3 \\ -8.5x_2 - 1.4512x_3 \\ -11x_3 \end{bmatrix}$	$-7.5489726x_1^2 - 8.5x_2^2 - 11x_3^2 < 0$	

Table 4 Proposed FOFLCs to stabilise chaos in FOPEMs in antecedent x_1

M_k	R_i	Consequent FOFLC	M_k	R_i	Consequent FOFLC
M_0	R_1	$U_1 = \begin{bmatrix} u_1 \\ u_2 \\ u_3 \end{bmatrix} = \begin{bmatrix} 0.0976x_3^2 - 0.045x_2x_3 + 5.912x_3 \\ -0.0107x_2^2 + 0.0237x_1x_2 - x_2 - 0.0041x_3 \\ -0.0108x_3^2 + 0.0147x_1x_3 - 0.0041x_1x_2 - x_3 \end{bmatrix}$	M_2	R_1	$U_1 = \begin{bmatrix} u_1 \\ u_2 \\ u_3 \end{bmatrix} = \begin{bmatrix} 0.1434x_3^2 - 0.0674x_2x_3 + 0.0025x_2^2 + 5.912x_3 \\ -0.0107x_2^2 + 0.0237x_1x_2 - x_2 - 1.4512x_3 \\ -0.0108x_3^2 + 0.0147x_1x_3 - 0.0041x_1x_2 - x_3 \end{bmatrix}$
	R_2	$U_2 = \begin{bmatrix} u_1 \\ u_2 \\ u_3 \end{bmatrix} = \begin{bmatrix} 0.0976x_3^2 - 0.045x_2x_3 + 5.912x_3 \\ -0.0107x_2^2 + 0.0237x_1x_2 - 8.5x_2 - 1.4512x_3 \\ -0.0108x_3^2 + 0.0147x_1x_3 - 0.0041x_1x_2 - x_3 \end{bmatrix}$		R_2	$U_2 = \begin{bmatrix} u_1 \\ u_2 \\ u_3 \end{bmatrix} = \begin{bmatrix} 0.1434x_3^2 - 0.0674x_2x_3 + 0.0025x_2^2 + 5.912x_3 \\ -0.0107x_2^2 + 0.0237x_1x_2 - 10.5x_2 - 1.4512x_3 \\ -0.0108x_3^2 + 0.0147x_1x_3 - 0.0041x_1x_2 - x_3 \end{bmatrix}$
	R_3	$U_3 = \begin{bmatrix} u_1 \\ u_2 \\ u_3 \end{bmatrix} = \begin{bmatrix} 0.0976x_3^2 - 0.045x_2x_3 + 5.912x_3 \\ -0.0107x_2^2 + 0.0237x_1x_2 - 8.5x_2 - 1.4512x_3 \\ -0.0108x_3^2 + 0.0147x_1x_3 - 0.0041x_1x_2 - 11x_3 \end{bmatrix}$		R_3	$U_3 = \begin{bmatrix} u_1 \\ u_2 \\ u_3 \end{bmatrix} = \begin{bmatrix} 0.1434x_3^2 - 0.0674x_2x_3 + 0.0025x_2^2 + 5.912x_3 \\ -0.0107x_2^2 + 0.0237x_1x_2 - 10.5x_2 - 1.4512x_3 \\ -0.0108x_3^2 + 0.0147x_1x_3 - 0.0041x_1x_2 - 13x_3 \end{bmatrix}$
M_1	R_1	$U_1 = \begin{bmatrix} u_1 \\ u_2 \\ u_3 \end{bmatrix} = \begin{bmatrix} 0.0976x_3^2 - 0.045x_2x_3 + 6.9174x_3 \\ -0.0107x_2^2 + 0.0237x_1x_2 - x_2 - 2.0814x_3 \\ -0.0213x_3^2 + 0.0255x_1x_3 - 0.0078x_1x_2 + 0.0013x_2^2 - x_3 \end{bmatrix}$	M_3	R_1	$U_1 = \begin{bmatrix} u_1 \\ u_2 \\ u_3 \end{bmatrix} = \begin{bmatrix} 0.0936x_3^2 - 0.0431x_2x_3 + 6.6007x_3 \\ -0.0103x_2^2 + 0.0227x_1x_2 - x_2 - 1.7263x_3 \\ -0.0318x_3^2 + 0.0355x_1x_3 - 0.005967x_1x_2 + 0.004x_1^2 + 0.00007x_2^2 - x_3 \end{bmatrix}$
	R_2	$U_2 = \begin{bmatrix} u_1 \\ u_2 \\ u_3 \end{bmatrix} = \begin{bmatrix} 0.0976x_3^2 - 0.045x_2x_3 + 6.9174x_3 \\ -0.0107x_2^2 + 0.0237x_1x_2 - 9.5x_2 - 2.0814x_3 \\ -0.0213x_3^2 + 0.0255x_1x_3 - 0.0078x_1x_2 + 0.0013x_2^2 - x_3 \end{bmatrix}$		R_2	$U_2 = \begin{bmatrix} u_1 \\ u_2 \\ u_3 \end{bmatrix} = \begin{bmatrix} 0.0936x_3^2 - 0.0431x_2x_3 + 6.6007x_3 \\ -0.0103x_2^2 + 0.0227x_1x_2 - 11.5x_2 - 1.7263x_3 \\ -0.0318x_3^2 + 0.0355x_1x_3 - 0.005967x_1x_2 + 0.004x_1^2 + 0.00007x_2^2 - x_3 \end{bmatrix}$
	R_3	$U_3 = \begin{bmatrix} u_1 \\ u_2 \\ u_3 \end{bmatrix} = \begin{bmatrix} 0.0976x_3^2 - 0.045x_2x_3 + 6.9174x_3 \\ -0.0107x_2^2 + 0.0237x_1x_2 - 9.5x_2 - 2.0814x_3 \\ -0.0213x_3^2 + 0.0255x_1x_3 - 0.0078x_1x_2 + 0.0013x_2^2 - 12x_3 \end{bmatrix}$		R_3	$U_3 = \begin{bmatrix} u_1 \\ u_2 \\ u_3 \end{bmatrix} = \begin{bmatrix} 0.0936x_3^2 - 0.0431x_2x_3 + 6.6007x_3 \\ -0.0103x_2^2 + 0.0227x_1x_2 - 11.5x_2 - 1.7263x_3 \\ -0.0318x_3^2 + 0.0355x_1x_3 - 0.005967x_1x_2 + 0.004x_1^2 + 0.00007x_2^2 - 14x_3 \end{bmatrix}$

Using the Lyapunov function in (21) and Lemma 1, we have (28).

$$D^\alpha V(x) \leq -(\varphi + \rho)x_1^2 - \beta x_2^2 - \gamma x_3^2 - \ldots - \tau x_n^2 \tag{28}$$

According to fractional-order Lyapunov stability theorem [20], $D^\alpha V(x) \leq 0$ indicates the system is stable.

The ASMC law used in the sliding surface so that $D^\alpha s(t) = 0$ is defined as in (29),

$$u = u_r + u_{eq} \tag{29}$$

where $u_r = \sigma \text{sgn}(s)$ is the reaching control law, σ is the reaching gain achieved by the adaptive law $\dot{\sigma} = -\emptyset|s|$; $\emptyset$ is a constant, and u_{eq} is the equivalent control law as in (30).

$$u_{eq} = D^\alpha x_1(t) - a(x_1, x_2, x_3, \ldots, x_n) + \varphi x_1 \tag{30}$$

Replacing $D^\alpha x_1(t)$ from (26) into (30), u_{eq} is obtained as (31).

$$\begin{aligned}
u_{eq} = &-x_2.b(x_1, x_2, x_3, \ldots, x_n) \\
&- x_3.c(x_1, x_2, x_3, \ldots, x_n) - \ldots \\
&- x_n.e(x_1, x_2, x_3, \ldots, x_n) - \rho x_1 \\
&- a(x_1, x_2, x_3, \ldots, x_n)
\end{aligned} \tag{31}$$

Therefore, ASMC u of (29) is obtained as in (32),

$$\begin{aligned}
u = &-x_2.b(x_1, x_2, x_3, \ldots, x_n) - x_3.c(x_1, x_2, x_3, \ldots, x_n) \\
&- \ldots - x_n.e(x_1, x_2, x_3, \ldots, x_n) - \rho x_1 \\
&- a(x_1, x_2, x_3, \ldots, x_n) + \sigma \text{sgn}(s)
\end{aligned} \tag{32}$$

where ρ, σ and s are to be suitably chosen.

Now, the above ASMC strategy is applied to the FOPEM M_0 (7).

$$\begin{cases}
D^\alpha x_1 = -0.0976x_3^2 + 0.045x_2x_3 - 7.5489726x_1 + u_1 \\
D^\alpha x_2 = 0.0107x_2^2 - 0.0237x_1x_2 \\
D^\alpha x_3 = 0.0108x_3^2 + 1.4512x_2 - 5.912x_1 \\
\quad -0.0147x_1x_3 + 0.0041x_1x_2
\end{cases} \tag{33}$$

Here, $u = (u_1, 0, 0)^T$, $u_1 = u_{r1} + u_{eq1}$ is the control signal.

Comparing system (33) with (23), we obtain (34).

$$\begin{cases}
a(x_1, x_2, x_3) = -0.0976x_3^2 + 0.045x_2x_3 \\
\varphi = 7.5489726 \\
b(x_1, x_2, x_3) = -0.0237x_2 \\
\beta = -0.0107x_2 \\
c(x_1, x_2, x_3) = -5.912 - 0.0147x_3 + 0.0041x_2 \\
d(x_1, x_2, x_3) = -1.4512 \\
\gamma = -0.0108x_3
\end{cases} \tag{34}$$

From (31) and (32), the ASMC u_1 is obtained as in (35).

$$\begin{aligned}
u_1 = &0.0237x_2^2 + 5.912x_3 + 0.01123x_3^2 - 0.0491x_2x_3 \\
&- \rho x_1 + \sigma sgn(s)
\end{aligned} \tag{35}$$

Suitable values of ρ, σ and s render the FOPEM, M_0 globally asymptotically stable. Similarly, the FOASMC for the chaotic FOPEMs, M_1, M_2 and M_3 are designed as given in Table 5.

3.1.1.3 FOABC: The recursive active backstepping control is designed for the ith step, where the ith-order sub-system is stabilised with respect to a Lyapunov function V_i and virtual control μ_i in the control input u_i.

Let, $w_1 = x_1$,

$$D^\alpha w_1 = D^\alpha x_1 = f_1(x(t), t) + u_1 \tag{36}$$

such that $x_2 = \mu_1(w_1)$ is the virtual control input.

To stabilise sub-system w_1, a Lyapunov function is chosen as in (37).

$$V_1 = \frac{w_1^2}{2} \tag{37}$$

Using FO Lemma 1, the Caputo fractional derivative of V_1 is obtained as in (38).

$$D^\alpha V_1 \leq w_1 D^\alpha w_1 = w_1[f_1(x(t), t) + u_1] \tag{38}$$

Considering $\mu_1 = 0$, an appropriate expression of u_1 is chosen such that $D^\alpha V_1 < 0$, and sub-system w_1 is asymptotically stable. The error between x_2 and μ_1 is given by (39).

$$w_2 = x_2 - \mu_1 \tag{39}$$

Therefore, the (w_1, w_2) sub-system is obtained, where $x_3 = \mu_2(w_1, w_2)$ is the virtual controller. The stabilisation of (w_1, w_2) sub-system is done by choosing a Lyapunov function, V_2 as in (40).

Table 5 Proposed FOASMC and FOABC to stabilise chaos in FOPEMs

FOPEM	Control technique	Parameter values	Controller
M_0	FOASMC	$\rho = 40$, $\sigma = 20$, $s = 8$	$u_1 = 0.0237x_2^2 + 5.912x_3 + 0.01123x_3^2 - 0.0491x_2x_3 - 40x_1 + 20\mathrm{sgn}(8)$
	FOABC	$w_1 = x_1$, $w_2 = x_2 - \mu_1$, $w_3 = x_3 - \mu_2$, $\mu_1 = \mu_2 = 0$	$u_1 = 0.0976x_3^2 - w_1,$ $u_2 = -0.0107w_2^2 + 0.0237w_1w_2 - w_2,$ $u_3 = -0.0108w_3^2 - 1.4512w_2 + 5.912w_1 + 0.0147w_1w_3 - 0.0041w_1w_2 - w_3 - 0.045w_1w_2$
M_1	FOASMC	$\rho = 50$, $\sigma = 20$, $s = 10$	$u_1 = 0.0237x_2^2 + 6.917x_3 + 0.1231x_3^2 - 0.0528x_2x_3 - 50x_1 + 20\mathrm{sgn}(10)$
	FOABC	$w_1 = x_1$, $w_2 = x_2 - \mu_1$, $w_3 = x_3 - \mu_2$, $\mu_1 = \mu_2 = 0$	$u_1 = 0.0976x_3^2 - w_1,$ $u_2 = -0.0107w_2^2 + 0.0237w_1w_2 - w_2,$ $u_3 = -0.0213w_3^2 - 2.0814w_2 + 6.9174w_1 + 0.0255w_1w_3 - 0.0528w_1w_2 + 0.0013w_2^2$
M_2	FOASMC	$\rho = 50$, $\sigma = 20$, $s = 5$	$u_1 = 0.0262x_2^2 + 5.912x_3 + 0.1581x_3^2 - 0.0715x_2x_3 - 50x_1 + 20\mathrm{sgn}(5)$
	FOABC	$w_1 = x_1$, $w_2 = x_2 - \mu_1$, $w_3 = x_3 - \mu_2$, $\mu_1 = \mu_2 = 0$	$u_1 = 0.1434x_3^2 - w_1,$ $u_2 = -0.0107w_2^2 + 0.0237w_1w_2 + 0.0025w_1w_2 - w_2,$ $u_3 = -0.0108w_3^2 - 1.4512w_2 + 5.912w_1 + 0.0147w_1w_3 - 0.0715w_1w_2 + w_3$
M_3	FOASMC	$\rho = 79$, $\sigma = 0.2$, $s = 0.2$	$u_1 = 0.0227x_2^2 + 6.6007x_3 + 0.1291x_3^2 - 0.049067x_2x_3 + 0.004x_1x_3 - 79x_1 + 0.2\mathrm{sgn}(0.2)$
	FOABC	$w_1 = x_1$, $w_2 = x_2 - \mu_1$, $w_3 = x_3 - \mu_2$, $\mu_1 = \mu_2 = 0$	$u_1 = 0.0936x_3^2 - w_1,$ $u_2 = -0.0103w_2^2 + 0.0227w_1w_2 - w_2,$ $u_3 = -0.049067w_1w_2 - 0.0318w_3^2 - 1.7263w_2 + 6.6007w_1 + 0.0355w_1w_3 + 0.004w_1^2 + (0.00007)w_2^2 - w_3$

$$V_2 = V_1 + \frac{w_2^2}{2} \tag{40}$$

Its Caputo derivative is as in (41).

$$D^\alpha V_2 \leq D^\alpha V_1 + w_2 D^\alpha w_2 = D^\alpha V_1 + w_2[f_2(x(t),t) + u_2] \tag{41}$$

Considering $\mu_2 = 0$, an appropriate expression of u_2 is chosen such that $D^\alpha V_2 < 0$, making (w_1, w_2) sub-system asymptotically stable.

Similarly, virtual controllers are designed for subsequent sub-systems $(w_1, w_2, \ldots, w_n)$, which are stabilised by choosing Lyapunov functions as in (42) and appropriate controller expressions.

$$V_i = V_{i-1} + \frac{w_i^2}{2} \tag{42}$$

If $D^\alpha V_i < 0$, for $i = 1, 2, \ldots, n.$, the controlled system (13) is asymptotically stable.

Now, we apply FOABC to FOPEM $M_0(7)$. From (36), we have,

$$D^\alpha w_1 = -7.5489726 w_1 - 0.0976 x_3^2 + 0.045 x_2 x_3. \tag{43}$$

From (38), we have (44).

$$D^\alpha V_1 = -7.5489726 w_1^2 + w_1 \left(-0.0976 x_3^2 + 0.045 \mu_1 x_3 w_1 + u_1\right) \tag{44}$$

$D^\alpha V_1 = -7.5489726 w_1^2 - w_1^2 < 0$, if $\mu_1 = 0$ and $u_1 = 0.0976 x_3^2 - w_1$, and sub-system w_1 is asymptotically stable.

From (41), we get,

$$D^\alpha V_2 = -7.5489726 w_1^2 - w_1^2 + 0.045 w_1 w_2 a_2 + w_2 \left(0.0107 w_2^2 - 0.0237 w_1 w_2 + u_2\right) \tag{45}$$

$D^\alpha V_2 = -7.5489726 w_1^2 - w_1^2 - w_2^2 < 0$, when $\mu_2 = 0$ and $u_2 = -0.0107 w_2^2 + 0.0237 w_1 w_2 - w_2$, and sub-system (w_1, w_2) is asymptotically stable.

Similarly, $D^\alpha V_3 = -8.5489726 w_1^2 + 0.045 w_1 w_2 w_3 + w_3 \left(0.0108 w_3^2 + 1.4512 w_2 - 5.912 w_1 - 0.0147 w_1 w_3 + 0.0041 w_1 w_2 + u_3\right) < 0$, and the sub-system (w_1, w_2, w_3) is asymptotically stable.

Thus, chaos in FOPEM M_0 is stabilised using FOABC. Similarly, the FOABC for remaining chaotic

FOPEMs, M_1, M_2 and M_3 are designed as enlisted in Table 5.

3.1.2 FO Controllers for synchronisation of chaos in FOPEMs

The controllers in this section are applied to two pairs:

a. Chaotic FOPEM M_0 acting as a slave synchronises with periodic FOPEM M_4 acting as a master
b. Chaotic FOPEM M_2 acting as a slave synchronises with periodic FOPEM M_5 acting as a master

Let the FO master system be a periodic system defined in (46).

$$D^\alpha y(t) = f(y(t), t) \tag{46}$$

where $y(t) = [y_1, y_2, \ldots, y_n]^T$ is the state vector, $y_i(0)$ represents the ICs and $i = 1, 2, \ldots, n.$ $f(y(t), t)) = [f_1(y), f_2(y), \ldots, f_n(y)]^T$ is an n-dimensional vector field containing continuous functions of the master system.

Let the FO slave system be a chaotic system defined in (47).

$$D^\alpha x(t) = f(x(t), t) + u \tag{47}$$

The errors between the master and slave are defined as in (48),

$$e = x - y \tag{48}$$

where $e = [e_1, e_2, \ldots, e_n]^T$ are the error states.
The FO error dynamics are obtained as in (49).

$$D^\alpha e = D^\alpha x - D^\alpha y \tag{49}$$

Therefore, the goal is to design u such that the error states converge to zero as time approaches infinity, i.e. the trajectory of the slave system (47) asymptotically approaches and synchronise with the trajectory of the master system (46).

Two control strategies for synchronisation are proposed in the following subsections: FO fuzzy logic synchronisation control (FOFLSC) and FO active backstepping synchronisation control (FOABSC).

3.1.2.1 FOFLSC: The ith fuzzy control rule for the FOFLSC is defined as in (50),

Rule i : IF e_1 is $E_{i,1}$ AND...AND e_n is $E_{i,n}$, THEN u_L
$$= u_i(e), i = 1, \ldots, r, r \in N^*$$
$$(50)$$

where $E_{i,1}, E_{i,2}, \ldots, E_{i,n}$ are fuzzy sets describing the LTs of input variables, $u_L = u_i(e)$ is the control input of rule i and r is the total number of fuzzy rules following the same defuzzification process as in Sect. 5.1.1.1.

The Lyapunov function is defined as in (51).

$$V(e) = \frac{1}{2}\left(e_1^2 + e_2^2 + e_3^2 + \ldots + e_n^2\right) \qquad (51)$$

From Theorem 2, it can be derived that if the origin is an equilibrium of the controlled system and $V(e) = \frac{1}{2}\left(e_1^2 + e_2^2 + e_3^2 + \ldots + e_n^2\right)$ is a positive definite function on domain E containing the origin of R^n such that $D^\alpha V(e) \leq 0$, for $i = 1, 2, \ldots, r$ and $e \in E$, and $S = \{e \in E : D^\alpha V(e) = 0\}$, and suppose no solution of (49) can stay identically in S except the trivial solution $e(t) \equiv 0$, then, the equilibrium at the origin is asymptotically stable in the domain E.

We now apply FOFLSC to synchronise FOPEM M_0 with M_4. The periodic FOPEM, M_4 is chosen as master and chaotic M_0 as slave. The error dynamics are given by (52).

$$\begin{cases} D^\alpha e_1 = -0.0976(x_3^2 - y_3^2) + 0.045(x_2 x_3 - y_2 y_3) \\ \quad -7.5489726 x_1 + 12.6237 y_1 + u_1 \\ D^\alpha e_2 = 0.0107(x_2^2 - y_2^2) - 0.0237(x_1 x_2 - y_1 y_2) + u_2 \\ D^\alpha e_3 = 0.0108(x_3^2 - y_3^2) + 1.4512 e_2 - 5.912 e_1 \\ \quad -0.0147(x_1 x_3 - y_1 y_3) + 0.0041(x_1 x_2 - y_1 y_2) + u_3 \end{cases}$$
$$(52)$$

u_{eq1}, u_{eq2} and u_{eq3} are selected as in (53).

$$\begin{cases} u_{eq1} = 0.0976(x_3^2 - y_3^2) - 0.045(x_2 x_3 - y_2 y_3) \\ \quad\quad + 7.5489726 x_1 - 12.6237 y_1 \\ u_{eq2} = -0.0107(x_2^2 - y_2^2) + 0.0237(x_1 x_2 - y_1 y_2) \\ u_{eq3} = -0.0108(x_3^2 - y_3^2) + 0.0147(x_1 x_3 - y_1 y_3) \\ \quad\quad -0.0041(x_1 x_2 - y_1 y_2) \end{cases}$$
$$(53)$$

From (49) and (50), we get

$$\begin{cases} D^\alpha e_1 = u_{L1} \\ D^\alpha e_2 = u_{L2} \\ D^\alpha e_3 = 1.4512 e_2 - 5.912 e_1 + u_{L3} \end{cases} \qquad (54)$$

and
$$E = [-1500, 1500] \times [-2500, 2000] \times [-800, 600].$$

From (51), the Lyapunov function is chosen as in (55).

$$V(e) = \frac{1}{2}\left(e_1^2 + e_2^2 + e_3^2\right) \qquad (55)$$

Using Caputo derivative, we have,

$$\begin{aligned} D^\alpha V(e) = e_1 u_{L1} + e_2 u_{L2} + 1.4512 e_2 e_3 - 5.912 e_1 e_3 \\ + e_3 u_{L3} \end{aligned}$$
$$(56)$$

Since, $D^\alpha V(e) = 0 \Leftrightarrow e = [0, 0, 0]^T$ which implies $S = \{0, 0, 0\}$. The fuzzy rules are derived as follows:

i. For Rule 1, R_1: for antecedent e_1 as P, we have the consequent as,

$$U_{L1} = \begin{bmatrix} u_{L1} \\ u_{L2} \\ u_{L3} \end{bmatrix} = \begin{bmatrix} -e_1 + 5.912 e_3 \\ -e_2 - 1.4512 e_3 \\ -e_3 \end{bmatrix}, \qquad \text{then}$$
$$D^\alpha V(e) = -e_1^2 - e_2^2 - e_3^2 < 0.$$

ii. For Rule 2, R_2: for antecedent e_1 as N, we have the consequent as,

$$U_{L2} = \begin{bmatrix} u_{L1} \\ u_{L2} \\ u_{L3} \end{bmatrix} = \begin{bmatrix} -6.5 e_1 + 5.912 e_3 \\ -9.5 e_2 - 1.4512 e_3 \\ -e_3 \end{bmatrix}, \qquad \text{then}$$
$$D^\alpha V(e) = -6.5 e_1^2 - 9.5 e_2^2 - e_3^2 < 0.$$

iii.

For Rule 3, R_3: for antecedent e_1 as Z, we have the consequent as

$$\begin{aligned} U_{L3} &= \begin{bmatrix} u_{L1} \\ u_{L2} \\ u_{L3} \end{bmatrix} \\ &= \begin{bmatrix} -6.5 e_1 + 5.912 e_3 \\ -9.5 e_2 - 1.4512 e_3 \\ -13 e_3 \end{bmatrix}, \text{ then } D^\alpha V(e) \\ &= -6.5 e_1^2 - 9.5 e_2^2 - 13 e_3^2 < 0 \end{aligned}$$

Thus, the errors, $e = [e_1, e_2, e_3]^T$, converge to zero and the slave M_0 synchronises with the master M_4. Similarly, the FOFLSC designed to synchronise FOPEMs, the chaotic M_2 with the periodic M_5 is as in Table 6.

3.1.2.2 FOABSC: The periodic FOPEM, M_4 is chosen as master and chaotic M_0 as slave. According to the design procedure mentioned in subsection 3.1.1.3, $e_3 = \mu_1(w_1)$ is the virtual control input. The

Table 6 Proposed TSFLSC for synchronisation in FOPEMs, M_0 (slave) with M_4 (master); and M_2 (slave) with M_5 (master) at antecedent e_1

Master system	Slave system	Rule i	Consequent synchronisation controller
M_4	M_0	R_1	$U_1 = \begin{bmatrix} 0.0976(x_3^2 - y_3^2) - 0.045(x_2x_3 - y_2y_3) + 7.5489726x_1 - 12.6237y_1 - e_1 + 5.912e_3 \\ -0.0107(x_2^2 - y_2^2) + 0.0237(x_1x_2 - y_1y_2) - e_2 - 1.4512e_3 \\ -0.0108(x_3^2 - y_3^2) + 0.0147(x_1x_3 - y_1y_3) - 0.0041(x_1x_2 - y_1y_2) - e_3 \end{bmatrix}$
		R_2	$U_2 = \begin{bmatrix} 0.0976(x_3^2 - y_3^2) - 0.045(x_2x_3 - y_2y_3) + 7.5489726x_1 - 12.6237y_1 - 6.5e_1 + 5.912e_3 \\ -0.0107(x_2^2 - y_2^2) + 0.0237(x_1x_2 - y_1y_2) - 9.5e_2 - 1.4512e_3 \\ -0.0108(x_3^2 - y_3^2) + 0.0147(x_1x_3 - y_1y_3) - 0.0041(x_1x_2 - y_1y_2) - e_3 \end{bmatrix}$
		R_3	$U_3 = \begin{bmatrix} 0.0976(x_3^2 - y_3^2) - 0.045(x_2x_3 - y_2y_3) + 7.5489726x_1 - 12.6237y_1 - 6.5e_1 + 5.912e_3 \\ -0.0107(x_2^2 - y_2^2) + 0.0237(x_1x_2 - y_1y_2) - 9.5e_2 - 1.4512e_3 \\ -0.0108(x_3^2 - y_3^2) + 0.0147(x_1x_3 - y_1y_3) - 0.0041(x_1x_3 - y_1y_3) - 13e_3 \end{bmatrix}$
M_5	M_2	R_1	$U_1 = \begin{bmatrix} 0.1434(x_3^2 - y_3^2) - 0.0674(x_2x_3 - y_2y_3) + 0.0025(x_2^2 - y_2^2) + 11.45376x_1 - 12.7264y_1 - e_1 + 5.912e_3 \\ -0.0107(x_2^2 - y_2^2) + 0.0237(x_1x_2 - y_1y_2) - e_2 - 1.4512e_3 \\ -0.0108(x_3^2 - y_3^2) + 0.0147(x_1x_3 - y_1y_3) - 0.0041(x_1x_2 - y_1y_2) - e_3 \end{bmatrix}$
		R_2	$U_2 = \begin{bmatrix} 0.1434(x_3^2 - y_3^2) - 0.0674(x_2x_3 - y_2y_3) + 0.0025(x_2^2 - y_2^2) + 11.45376x_1 - 12.7264y_1 - 7.5e_1 + 5.912e_3 \\ -0.0107(x_2^2 - y_2^2) + 0.0237(x_1x_2 - y_1y_2) - 10.5e_2 - 1.4512e_3 \\ -0.0108(x_3^2 - y_3^2) + 0.0147(x_1x_3 - y_1y_3) - 0.0041(x_1x_2 - y_1y_2) - e_3 \end{bmatrix}$
		R_3	$U_3 = \begin{bmatrix} 0.1434(x_3^2 - y_3^2) - 0.0674(x_2x_3 - y_2y_3) + 0.0025(x_2^2 - y_2^2) + 11.45376x_1 - 12.7264y_1 - 7.5e_1 + 5.912e_3 \\ -0.0107(x_2^2 - y_2^2) + 0.0237(x_1x_2 - y_1y_2) - 10.5e_2 - 1.4512e_3 \\ -0.0108(x_3^2 - y_3^2) + 0.0147(x_1x_3 - y_1y_3) - 0.0041(x_1x_2 - y_1y_2) - 15e_3 \end{bmatrix}$

Table 7 Proposed FOABSC for synchronisation in FOPEMs, M_0 (slave) with M_4 (master); and M_2 (slave) with M_5 (master)

Master system	Slave system	Parameter values	FOABSC
M_4	M_0	$w_1 = e_1,$ $w_2 = e_2 - \mu_2,$ $w_3 = e_3 - \mu_1,$ $\mu_1 = \mu_2 = 0$	$u_1 = 0.045(x_2x_3 - y_2y_3) - 5.074727y_1 - w_1,$ $u_2 = -0.0107w_2w_3 + 0.0237(x_1x_2 - y_1y_2) + 1.4512w_3 - w_2,$ $u_3 = 0.0976(y_3 + x_3)w_1 - 0.0108(y_3 + x_3)w_3 + 5.912w_1 + 0.0147(x_1x_3 - y_1y_3) - 0.0041(x_1x_2 - y_1y_2) - w_3$
M_5	M_2	$w_1 = e_1,$ $w_2 = e_2 - \mu_2,$ $w_3 = e_3 - \mu_1,$ $\mu_1 = \mu_2 = 0$	$u_1 = 0.0025e_2(y_2 + x_2) - 0.0674(x_2x_3 - y_2y_3) - 1.27264y_1 - w_1,$ $u_2 = -1.4512w_3 - 0.0107(y_2 + x_2)w_2 + 0.0237(x_1x_2 - y_1y_2) - w_2,$ $u_3 = 0.1434(y_3 + x_3)w_1 - 0.0108(y_3 + x_3)w_3 - 5.912w_1 - 0.0147(x_1x_3 - y_1y_3) - 0.0041(x_1x_2 - y_1y_2) - w_3$

Lyapunov function is chosen as in (37) and its FO derivative is as in (57).

$$D^{\alpha}V_1 = -7.5489726w_1^2 + w_1(-0.0976(y_3 + x_3)\mu_1 \\ + 0.045(x_2x_3 - y_2y_3) + 5.0747274y_1 + u_1) \tag{57}$$

$D^{\alpha}V_1 = -7.5489726w_1^2 - w_1^2 < 0$, i.e. sub-system w_1 is asymptotically stable when $\mu_1 = 0$ and $u_1 = 0.045(x_2x_3 - y_2y_3) - 5.074727y_1 - w_1$.

For the Lyapunov function, V_2 in (58), we get its FO derivative in (59).

$$V_2 = V_1 + \frac{z_3^2}{2} \tag{58}$$

$$D^{\alpha}V_2 = -8.5489726w_1^2 - 0.0976(y_3 + x_3)w_1w_3 \\ + w_3(0.0108(y_3 + x_3)w_3 + 1.4512\mu_2 \\ -5.912w_1 - 0.0147(x_1x_3 - y_1y_3) \\ + 0.0041(x_1x_2 - y_1y_2) + u_3) \tag{59}$$

$D^{\alpha}V_2 = -8.5489726w_1^2 - w_3^2 < 0$, when $\mu_2 = 0$ and $u_3 = 0.0976(y_3 + x_3)w_1 - 0.0108(y_3 + x_3)w_3 + 5.912w_1 + 0.0147(x_1x_3 - y_1y_3) - 0.0041(x_1x_2 - y_1y_2) - w_3$, which makes sub-system (w_1, w_3) asymptotically stable.

Similarly, $D^{\alpha}V_3 = -8.5489726w_1^2 - w_3^2 - w_2^2 < 0$, which makes (w_1, w_2, w_3) sub-system asymptotically stable.

Therefore, the synchronisation errors $e = [e_1, e_2, e_3]^{\mathrm{T}}$ converge to zero and the controlled system, i.e. chaotic FOPEM M_0 asymptotically approaches the trajectory of the periodic master system, FOPEM M_4. Similarly, FOABSC is designed to synchronise chaotic FOPEM, M_2 with periodic FOPEM, M_5 as shown in Table 7.

3.2 FO cancer epidemic model (FOCEM)

The proposed FOCEM is given as in (60), where x_1, x_2 and x_3 represent the tumour cell population, numbers of healthy cells and effector immune population, respectively. The IOM for the same was reported in Valle et al. [81].

$$\begin{cases} D^{\alpha}x_1 = x_1(1 - x_1) - a_{12}x_1x_2 - a_{13}x_1x_3 \\ D^{\alpha}x_2 = r_2x_2(1 - x_2) - a_{21}x_1x_2 \\ D^{\alpha}x_3 = \dfrac{r_2x_1x_3}{x_1 + 1} - a_{31}x_1x_3 - d_3x_3 \end{cases} \tag{60}$$

Here, a_{12} denotes fractional tumour cells killed by healthy cells, a_{13} is fractional tumour cells killed by effector cells, r_2 is healthy host cells growth rate, a_{21} denotes fractional healthy cells killed by tumour cells, a_{31} denotes fractional effector cells inactivated by tumour cells, d_3 denotes death rate of effector cells Valle et al. [81]. The phase solutions of the above system (60) with the parameter set $\{a_{12} = 1, a_{13} = 2.5, \quad r_2 = 4.5, a_{21}=1.5, a_{31} = 0.2, d_3 = 0.5\}$ give rise to chaos [36]. The dynamical analysis of the FOCEM is given in Table 8.

The phase portraits of the FOCEM (60) in Fig. 4 confirm that they are chaotic in nature in their fractional dynamics.

3.2.1 FO Controllers for stabilisation of chaos in FOCEM

Using the design procedure discussed in Section 3.1.1.1, the FOFLCs for stabilising chaos in the FOCEM are given in Table 9.

Similarly, using the design procedure discussed in Sects. 3.1.1.2 and 3.1.1.3, the FOASMC and FOABC for stabilising chaos in the FOCEM are given in Table 10.

Having designed the controllers for stabilisation and synchronisation in FOPEMs and FOCEM, we now proceed to their results, discussion and comparison.

4 Comparison of the FOCs in FOPEMs and FOCEM

Comparisons of stabilisation and synchronisation FOCs are presented in the following two subsections.

4.1 Comparison of the FOCs to stabilise chaos

The numerical simulation results of FOFLC, FOASMC and FOABC applied to the epidemics FOPEMs and FOCEM as designed in Sects. 3.1.1 and 3.2.1 to stabilise chaos are shown in Figs. 5, 6, 7, 8 and 9. A comparison is drawn in Table 11 where 'state' denotes the number of state variables controlled.

From Table 11, it is noted that FOFLC is the fastest controller in terms of settling time, while FOASMC requires the least control effort to stabilise chaos. The

Table 8 Investigation of dynamics of FOCEM

Epidemic	ICs	Equilibrium points	Eigen values $(\lambda_i, i = 1, 2, 3)$	FO	LEs	Observation
Cancer	(0.1,0.1,0.1)	$E_1 = (0,0,0)$	$\lambda_{1,2,3} = (-1/2, 3/5, 1)$	0.99	$LE_1 = 0.013852$	Chaotic
		$E_2 = (1,0,0)$	$\lambda_{1,2,3} = (-1, -9/10, 31/20)$		$LE_2 = 0$	
		$E_3 = (0,1,0)$	$\lambda_{1,2,3} = (-3/5, -1/2, 0)$		$LE_3 = -0.52734$	

Table 9 Proposed FOFLC to stabilise chaos in FOCEM in antecedent x_1

Epidemic	FO	Fuzzy rules	FOFLC
FOCEM	0.99	Rule 1	$U_1 = \begin{bmatrix} u_1 \\ u_2 \\ u_3 \end{bmatrix} = \begin{bmatrix} x_1 x_2 + 2.5 x_1 x_3 - x_1 \\ 1.5 x_1 x_2 - x_2 \\ -\dfrac{4.5 x_1 x_3}{x_1 + 1} + 0.2 x_1 x_3 \end{bmatrix}$
		Rule 2	$U_2 = \begin{bmatrix} u_1 \\ u_2 \\ u_3 \end{bmatrix} = \begin{bmatrix} x_1 x_2 + 2.5 x_1 x_3 - 2x_1 \\ 1.5 x_1 x_2 - x_2 \\ -\dfrac{4.5 x_1 x_3}{x_1 + 1} + 0.2 x_1 x_3 \end{bmatrix}$
		Rule 3	$U_3 = \begin{bmatrix} u_1 \\ u_2 \\ u_3 \end{bmatrix} = \begin{bmatrix} x_1 x_2 + 2.5 x_1 x_3 - 2x_1 \\ 1.5 x_1 x_2 - 3x_2 \\ -\dfrac{4.5 x_1 x_3}{x_1 + 1} + 0.2 x_1 x_3 \end{bmatrix}$

designed controllers stabilise chaos in these models, and further illustrate that taking appropriate measures to reduce the number of infected rats will bring about a reduction in disease propagation. The proposed control strategies for chaos stabilisation may be accomplished by an efficient route of human action through medical intervention to methodically slow down the disease spread. The FOCEM stabilised using the proposed FOCs highlight the importance of maximum recruitment rate of effector cells being stronger than their inactivation rate by Cancer cells, on failure of which, necessary treatment is to be delivered to control tumour growth. In order to bring about zero tumour survival, the designed controllers aim at controlling the parameter assigned as fractional tumour cells killed by healthy cells.

4.2 Comparison of the FOCs to synchronise chaos

The numerical simulation results of applying the controllers FOFLSC and FOABSC for synchronisation as designed in Sect. 3.1.2 are shown in Figs. 10 and 11.

Chaotic models have a degree of unpredictability. The purpose of synchronisation is to synchronise the chaotic dynamical model with that of an unchaotic or periodic model so that the system is no longer chaotic, and the unpredictability in the epidemic spread is mitigated. As shown in Figs. 10 and 11, the error states $E = [e_1, e_2, e_3]^T$ converge to zero and the controlled slave system asymptotically approaches the trajectory of the master system. The comparison drawn in Table 12 reveal that FOFLSC is faster than FOABSC. Since our models are chaotic and strongly sensitive to ICs, we analyse the robustness of the control of the proposed models by perturbing the models with different ICs. Then, the corresponding integral squared error $ISE = \int_0^T e^2(t)dt$ is computed after application of the same control action. The results obtained are listed in Tables 11 and 12 which prove that the control strategies applied to the proposed models are robust, since the controllers are successful in attaining the desired stabilisation dynamics even after perturbation in the ICs. Such robustness provides a good argument for the controllers to be effective in suppressing and synchronising chaos in the proposed models.

Table 10 Proposed controllers FOASMC and FOABC to stabilise chaos in FOCEM

Epidemic	Control technique	FO	Parameter values	Controller
FOCEM	FOASMC	0.99	$\rho = 800,$ $\sigma = 0.5,$ $s = 0.5$	$u = 1.5x_2^2 - \frac{4.5x_3^2}{x_1+1} + 0.2x_3^2 + x_1^2 + x_1x_2 + 2.5x_1x_3 - 800x_1 + 0.5\text{sgn}(0.5)$
	FOABC	0.99	$w_1 = x_1,$ $w_2 = x_2 - \mu_1,$ $w_3 = x_3 - \mu_2,$ $\mu_1 = \mu_2 = 0$	$u_1 = -w_1 + 2.5w_1x_3,$ $u_2 = -w_2 + 0.6w_2^2 + 1.5w_1w_2 + w_1,$ $u_3 = -\frac{4.5w_1w_3}{w_1+1} + 0.2w_1w_3$

4.3 FO Covid-19 pandemic model (FOCovM)

The IOM of chaotic Covid-19 pandemic model is reported in Mangiarotti et al. [53]. The FOCovM is proposed in (61).

$$\begin{cases} D^\alpha x_1 = -0.10530723x_3^2 + 2.343 \times 10^{-5}x_1^2 \\ \qquad -0.15204x_2(x_3 - 0.01451520x_1) \\ D^\alpha x_2 = -0.20517824x_1 + 0.44040714x_2 + 0.16060376x_3^2 \\ D^\alpha x_3 = -0.00011493x_1x_3 - 1.215 \times 10^{-5}x_1x_2 \\ \qquad +0.2844499x_3 + 2.38 \times 10^{-6}x_1x_2 \end{cases}$$
(61)

where x_1, x_2, x_3 are the numbers of confirmed cases, critical cases under intensive care and cumulated number of fatalities per day, respectively.

The bifurcation diagram shown in Fig. 12 reveals the rich complex dynamics of Covid-19 pandemic as it progresses on increasing the FO parameter α in (61), which otherwise remain concealed in the IO chaotic model. The FOCovM displays a period 1 attractor (P1), in the range $\alpha\epsilon[0.95, 0.96]$, and bifurcates in two curves to give birth to a period 2 attractor (P2), in [0.96, 0.97]. On further splitting, P2 bifurcates into P4 (period 4) which eventually routes to chaos from $\alpha = 0.973$ onwards.

The phase portraits of the FOCovM shown in Fig. 13 illustrate the gradual evolution of the chaotic attractor at $\alpha = 0.98$ from a P1 at $\alpha = 0.95$, complying with the bifurcation analysis of Fig. 12.

The design of controllers in the FOCovM for stabilisation of chaos to a disease-free equilibrium or synchronisation of the chaotic trajectory with a disease-free one is left open to interested researchers. The review carried out in this paper highlights the research gaps in epidemic modelling and control and leads to focus on some unexplored areas that may be a scope of research:

1. FO chaos theory in modelling pandemics: The spread of pandemics such as COVID-19 is deterministic chaos having long-range memory. The present existing IO chaotic models are memory-less models. Chaos theory along with the memory-enabled fractional calculus can be a promising tool in modelling these epidemic/pandemics by capturing real, physical and unmodelled dynamics compared to IOMs. Also the FOMs are capable of presenting more robust models compared to their IO counterparts [49, 50]

2. FO chaos theory in decision-making: The investigation of FO models and their analysis of propagation can be applied to other infected regions to help recognise the closest scenarios to predict the future behaviour of the course of the epidemic. These will serve as an efficient tool in decision making [53] to generate an early alert system and aid in adopting economic control strategies of vaccination, ICU facility, etc., especially in low-income countries with limited health infrastructure.

3. FO chaos theory in destination crisis management: Chaos theory provides a viable framework for the management of disaster in countries whose income is largely dependent on tourism [72] as was the case with the H1N1 influenza crisis in Mexico. FO chaos theory can be a new tool to define tourism crisis.

4. FO controllers for FO chaotic epidemics: In an epidemic governed by chaotic behaviour, a seemingly trivial event may initiate a set of events leading to a major crisis. FO controllers provide robust stability conditions for uncertain chaotic systems [17]. Compared with their IO counterparts, FOCs have more flexibility in choosing the suitable control parameters to control and stabilise the chaotic equilibrium to an infection-free equilibrium. This is another scope of research since such wide range of flexibility of FOCs will enhance adopting preventive control measure in a
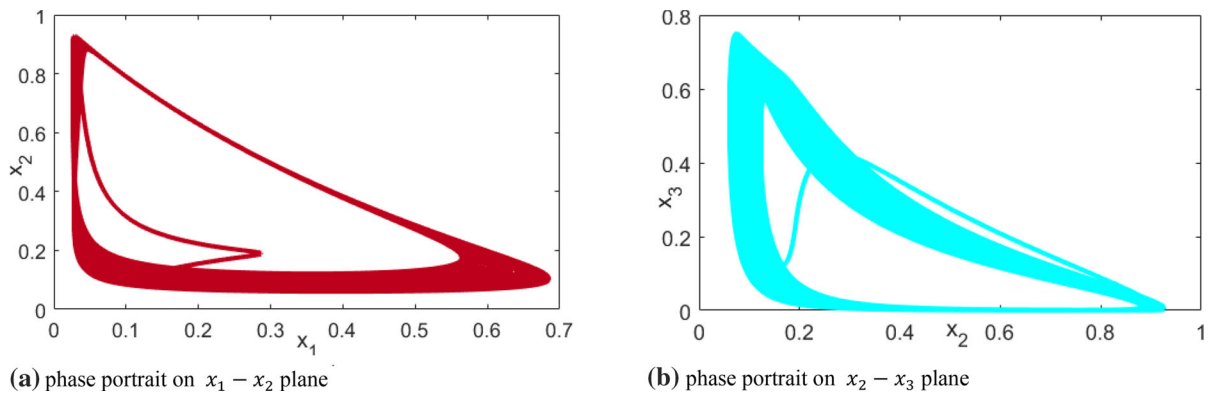
(a) phase portrait on $x_1 - x_2$ plane   **(b)** phase portrait on $x_2 - x_3$ plane

Fig. 4 Chaotic attractors of proposed FO Cancer epidemic model at $\alpha = 0.993$

(a) FOFLC   **(b)** FOASMC   **(c)** FOABC
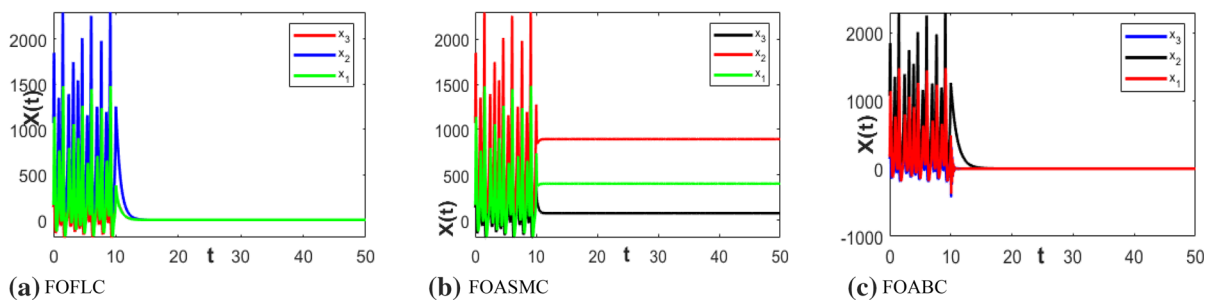
Fig. 5 Chaos stabilisation in FO Plague epidemic model, M_0 at $\alpha = 0.98$

(a) FOFLC   **(b)** FOASMC   **(c)** FOABC
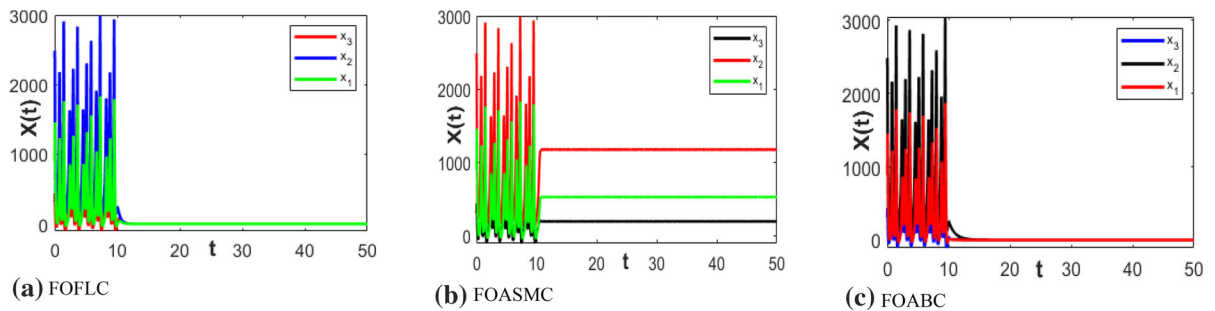
Fig. 6 Chaos stabilisation in FO Plague epidemic model M_1 at $\alpha = 0.98$

rapidly propagating epidemic. As an instance, the design of FOCs for stabilising and synchronising chaos in the ongoing chaotic Covid-19 model dynamics may be explored.

5 Conclusions

This brief survey reveals that chaotic waves are a dominant mode of epidemic/pandemic dispersal. Fractional calculus, possessing the features of flexibility, heredity and memory, can provide more accurate models of the chaotic pandemics by incorporating
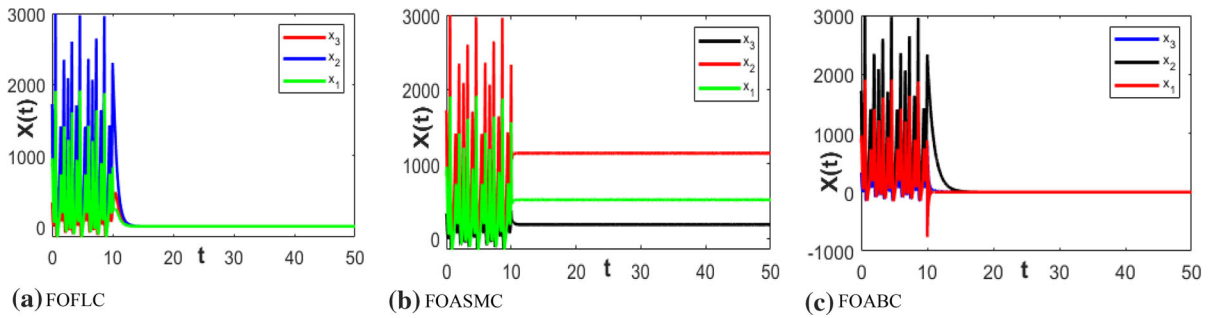
Fig. 7 Chaos stabilisation in FO Plague epidemic model M_2 at $\alpha = 0.995$
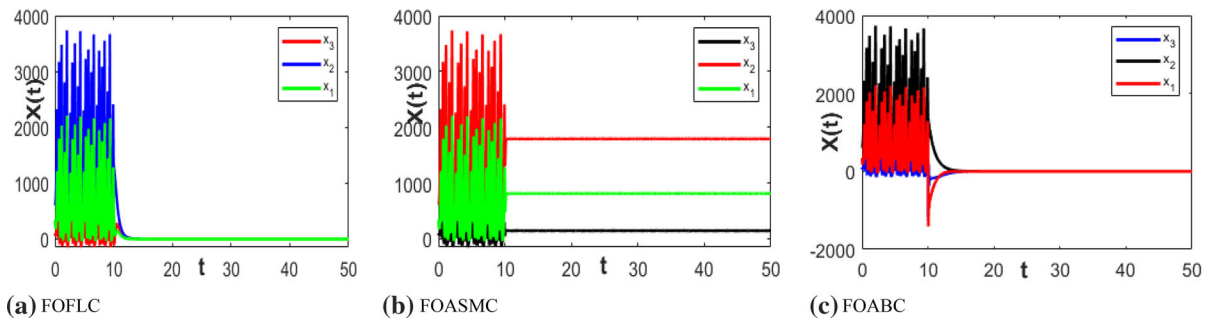

Fig. 8 Chaos stabilisation in FO Plague epidemic model M_3 at $\alpha = 0.995$
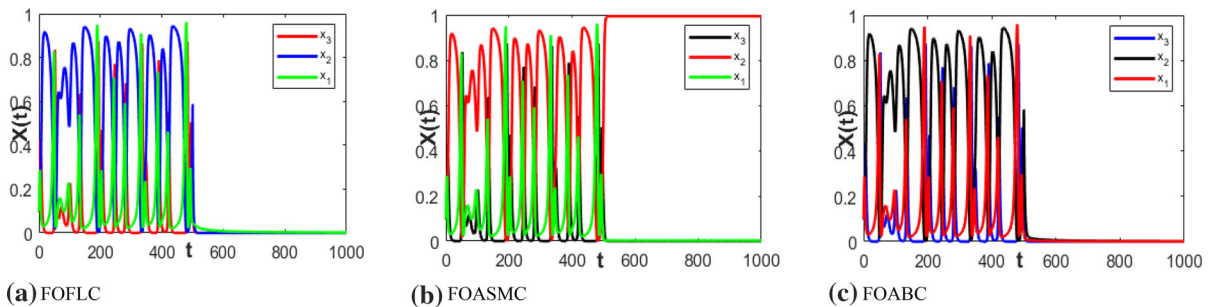

Fig. 9 Chaos stabilisation in FO Cancer epidemic model at $\alpha = 0.99$

unmodelled dynamics as ultra-diffusive, undetected or asymptomatic transmission, critical cases with comorbidities, etc., that often fail to be encompassed by integer-order models. A conclusion drawn is that on applying fractional-order chaos to model Plague, Cancer and Covid-19 pandemics based on actual data, realistic transmission revealing in-depth insights to their propagation dynamics such as asymptotically periodic attractors that evolve into chaos is discovered. The stability of the disease-free equilibrium is

achieved and synchronised using fractional-order control. The designed controllers in practical scenario may denote controlling the number of infected rats in Plague model, rate of recruitment of effector cells in Cancer model, injection of vaccine and prophylactic drug to susceptible individuals, social distancing, restriction of mobility, prior prediction of spread, etc., in Covid-19 model. Knowledge of propagation dynamics of pandemics as studied in this work facilitate judicious decision-making on timely and

Table 11 Comparison of the FOCs designed to stabilise chaos in FOPEMs and FOCEM

Epidemic	FOC	State	Settling time (t_s) (s)	Convergence to equilibrium point	Original ICs	Perturbed ICs	ISE
FOPEM M_0	FOFLC	3	3.24	E_2(Fig. 5a)	(166.8903,	(100, 1000,100)	0.04
	FOASMC	1	5.41	E_3(Fig. 5b)	1070.193,		0.34
	FOABC	3	6.23	E_2(Fig. 5c)	138.7208)		0.152
FOPEM M_1	FOFLC	3	1.46	E_1(Fig. 6a)	(895.9957,	(200, 2000, 300)	0.0004
	FOASMC	1	4.12	E_3(Fig. 6b)	2391.688,		0.025
	FOABC	3	4.81	E_1(Fig. 6c)	312.7087)		0.25
FOPEM M_2	FOFLC	3	3.42	E_1(Fig. 7a)	(836.9658,	(900,1000,400)	0.176
	FOASMC	1	4.7	E_3(Fig. 7b)	1721.620,		0.0061
	FOABC	3	6.72	E_1(Fig. 7c)	328.9299)		0.42
FOPEM M_3	FOFLC	3	3.39	E_3(Fig. 8a)	(344.0896,	(200, 500, 100)	0.425
	FOASMC	1	5.52	E_1(Fig. 8b)	627.7882,		0.0023
	FOABC	3	6.41	E_3(Fig. 8c)	101.5058)		0.419
FOCEM	FOFLC	3	25.8	E_1(Fig. 9a)	(0.1,0.1,0.1)	(10,10,10)	0.0049
	FOASMC	1	59	E_3(Fig. 9b)			0.3868
	FOABC	3	61.5	E_1(Fig. 9c)			0.057

(a) x_1 synchronises with y_1 using FOFLSC

(b) Synchronisation errors on using FOFLSC

(c) x_1 synchronises with y_1 using FOABSC

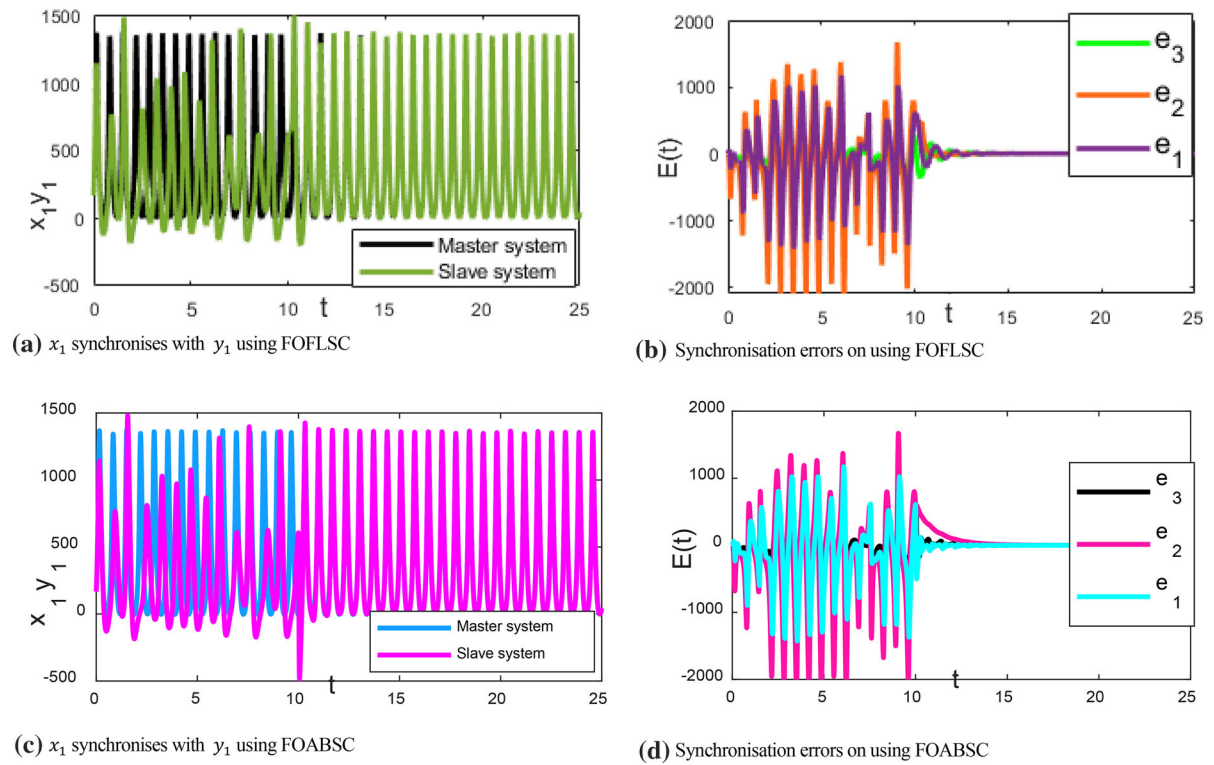**(d)** Synchronisation errors on using FOABSC

Fig. 10 Synchronisation control for FOPEMs, M_4(master) and M_0(slave)

Table 12 Comparison of the FOCs designed to synchronise chaos in FOPEMs

Master system	Slave system	Controller	State	Error settling time (t_s) (s)	Original ICs	Perturbed ICs	ISE
M_4	M_0	FOFLSC	3	5.52	(166.8903,	(100, 1000, 100)	0.81
		FOABSC	3	6.15	1070.193, 138.7208)		0.16
M_5	M_2	FOFLSC	3	6.61	(836.9658,	(700, 1800, 420)	0.49
		FOABSC	3	8.63	1721.620, 328.9299)		1.04

(a) x_1 synchronises with y_1 using FOFLSC

(b) Synchronisation errors on using FOFLSC

(c) x_1 synchronises with y_1 using FOABSC

(d) Synchronisation errors on using FOABSC
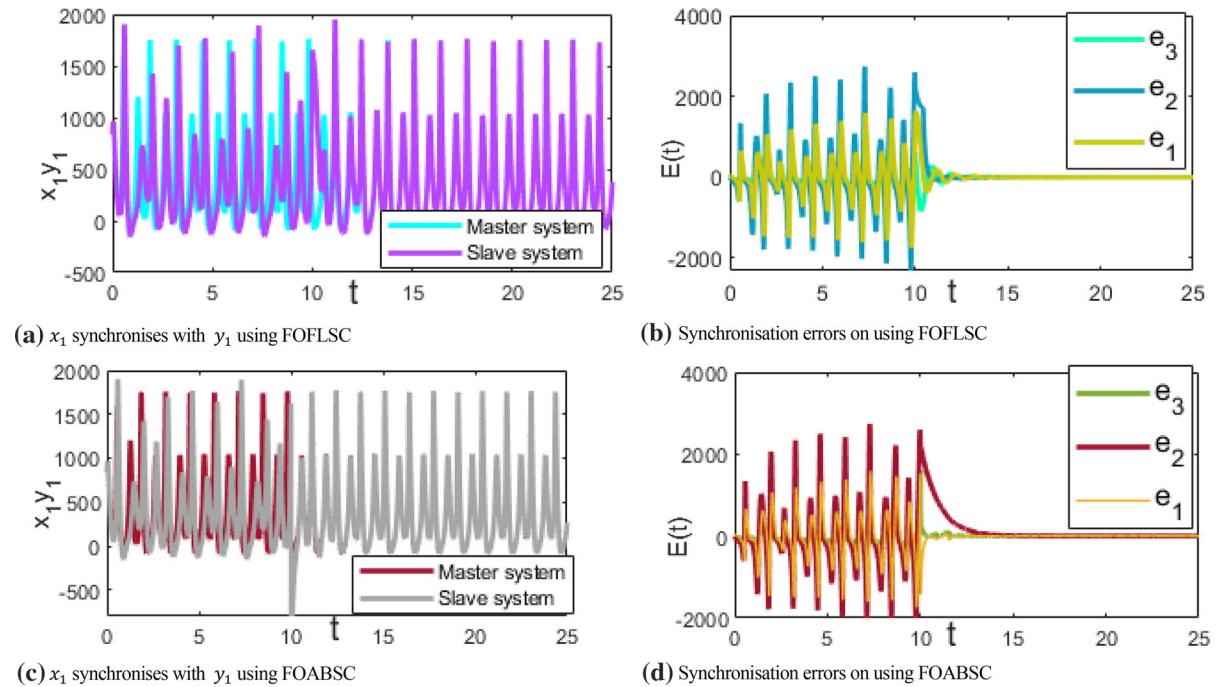
Fig. 11 Synchronisation control for FOPEMs, M_5(master) and M_2(slave)
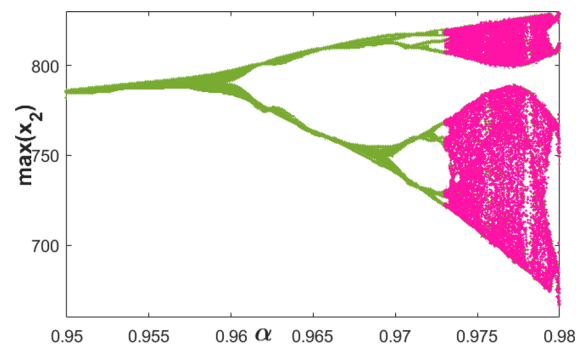
Fig. 12 Bifurcation of Covid-19 pandemic model against the FO parameter α

cost-effective control measures in low- and middle-income countries like India, which is struggling to battle the second wave of Covid-19 due to limited medical infrastructure: shortage of vaccines, oxygen supply, ICU beds, etc. Chaos and its unpredictability increase as FO operator increases; hence, it can be used as a parameter to analyse the progression of a pandemic and is an excellent tool to obtain a closer fit to the disease dynamics. It is to be noted that since chaos indicates hyped sensitivity to initial conditions, so a long-term prediction of the spread of the epidemic is never possible and substantial changes may occur unexpectedly. Nonetheless, this review will prove helpful to design quicker control measures to
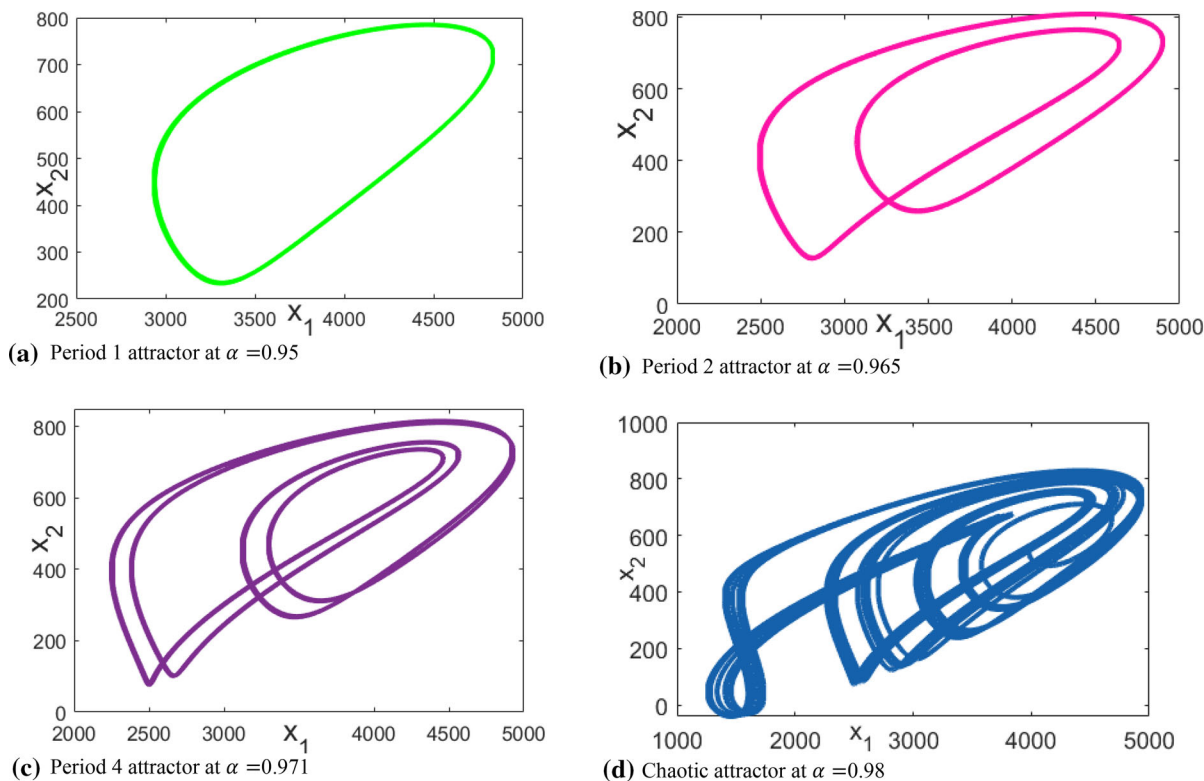
(a) Period 1 attractor at $\alpha = 0.95$

(b) Period 2 attractor at $\alpha = 0.965$

(c) Period 4 attractor at $\alpha = 0.971$

(d) Chaotic attractor at $\alpha = 0.98$

Fig. 13 Phase portraits of FO Covid-19 pandemic model

eliminate chaos, induce crisis management and decision-making in the pandemic using the more realistic approach of fractional-order chaos theory and thus curtail the unpredictability in the spread of the disease.

Data availability The datasets generated during and/or analysed during the current study are available from the corresponding author on reasonable request.

Conflict of interest The authors declare that they have no conflict of interest.

References

1. Abdelaziz, M.A.M., Ismail, A.I., Adbullah, F.A., Mohd, M.H.: Bifurcations and chaos in a discrete SI epidemic model with fractional order. Adv. Differ. Equ. (2018). https://doi.org/10.1186/s13662-018-1481-6

2. Aguiar, M., Stollenwerka, N., Kooi, B.W.: Torus bifurcations, isolas and chaotic attractors in a simple dengue fever model with ADE and temporary cross immunity. Int. J. Comput. Math. **86**, 1867–1877 (2009)

3. Aguila-Camacho, N., Duarte-Mermoud, M.A., Gallegos, J.A.: Lyapunov functions for fractional order systems. Commun. Nonlinear Sci. Numer. Simul. **19**, 2951–2957 (2014)

4. Agusto, F.B., Khan, M.A.: Optimal control strategies for dengue transmission in Pakistan. Math. Biosci. **305**, 102–121 (2018)

5. Ahmed, E., Elgazzar, A.S.: On fractional order differential equations model for nonlocal epidemics. Physica A **379**, 607–614 (2007)

6. Ansari, S.P., Agrawal, S.K., Das, S.: Stability analysis of fractional-order generalized chaotic susceptible-infected-recovered epidemic model and its synchronization using active control method. Pramana J. Phys. **84**, 23–32 (2015)

7. Bacaër, N.: The model of Kermack and McKendrick for the plague epidemic in Bombay and the type reproduction number with seasonality. J. Math. Biol. **64**, 403–422 (2012)

8. Bairagi, N., Adak, D.: Dynamics of cytotoxic T-lymphocytes and helper cells in human immunodeficiency virus infection with Hill-type infection rate and sigmoidal CTL expansion. Chaos Solitons Fractals **103**, 52–67 (2017)

9. Berhe, H.W., Qureshi, S., Shaikh, A.A.: Deterministic modeling of dysentery diarrhoea epidemic under fractional Caputo differential operator via real statistical analysis.

Chaos Solitons Fractals (2019). https://doi.org/10.1016/j.chaos.2019.109536

10. Berhe, H.W.: Optimal control strategies and cost-effectiveness analysis applied to real data of cholera outbreak in Ethiopia's Oromia region. Chaos Solitons Fractals **138**, 109933 (2020). https://doi.org/10.1016/j.chaos.2020.109933

11. Borah, M.: On coexistence of fractional-order hidden attractors. J. Comput. Nonlinear Dyn. **13**, 090906–090917 (2018). https://doi.org/10.1115/1.4039841

12. Borah, M., Das, D., Gayan, A., Fenton, F., Cherry, E.: Control and anticontrol of chaos in Fractional-order models of Diabetes, HIV, Dengue, Migraine, Parkinson's and Ebola Virus diseases. Chaos Solitons Fractals **153**, 111419 (2021). https://doi.org/10.1016/j.chaos.2021.111419

13. Borah, M., Roy, B.K.: Fractional-order systems with diverse dynamical behaviour and their switching-parameter hybrid-synchronisation. Eur. Phys. J. Spec. Top. **226**, 3747–3773 (2017). https://doi.org/10.1140/epjst/e2018-00063-9

14. Borah, M., Roy, B. K.: A Novel Multi-wing Fractional-order Chaotic System, its synchronisation control and application in secure communication. In: IEEE International Conference on Energy, Power and Environment (ICEPE), NIT Meghalaya, India, pp. 1–6. (2018). https://doi.org/10.1140/epjst/e2018-00063-9

15. Borah, M., Roy, B.K.: Systematic construction of high dimensional fractional-order hyperchaotic systems. Chaos Solitons Fractals (2020). https://doi.org/10.1016/j.chaos.2019.109539

16. Borah, M., Roy, B.K., Kapitaniak, T., Rajagopal, K., Volos, C.: A revisit to the past plague epidemic (India) versus the present COVID-19 pandemic: fractional-order chaotic models and fuzzy logic control. Eur. Phys. J. Spec. Top. (2021). https://doi.org/10.1140/epjs/s11734-021-00335-2

17. Boudjehem, D., Boudjehem, B.: Robust fractional order controller for chaotic systems. IFAC-PapersOnLine. **49**, 175–179 (2016)

18. Brady, O., Gething, P., Bhatt, S., Messina, J., Brownstein, J., Hoen, A., Moyes, C., Farlow, A., Scott, T., Hay, S.: Refining the global spatial limits of dengue virus transmission by evidence-based consensus. PLoS Negl. Trop. Dis. (2012). https://doi.org/10.1371/journal.pntd.0001760

19. British broadcasting corporation (2021) Black fungus: India reports nearly 9,000 cases of rare infection. https://www.bbc.com/news/world-asia-india-57217246

20. Chen, D., Zhang, R., Liu, X., Ma, X.: Fractional order Lyapunov stability theorem and its applications in synchronization of complex dynamical networks. Commun. Nonlinear Sci. Numer. Simul. **19**, 4105–4121 (2014)

21. Chang, C., Jing, Y.: T-S fuzzy modeling and control for a class of epidemic system with nonlinear incidence rates. In: 4th International Conference on Information, Cybernetics and Computational Social Systems (ICCSS), Dalian, pp. 154–159 (2017). https://doi.org/10.1109/ICCSS.2017.8091403

22. Chang, C., Jing, Y., Zhu, B.: Modeling and control for a descriptor epidemic system with nonlinear incidence rates. In: 30th Chinese Control and Decision Conference (CCDC). IEEE (2018). https://doi.org/10.1109/CCDC.2018.8407488

23. Chen, J.G., Zhang, S.W.: Liver cancer epidemic in China: past, present and future. Semin. Cancer Biol. **21**, 59–69 (2011)

24. Dangbe, E., Irepran, D., Perasso, A., Bekolle, D.: Mathematical modelling and numerical simulations of the influence of hygiene and seasons on the spread of cholera. Math. Biosci. (2017). https://doi.org/10.1016/j.mbs.2017.12.004

25. Dastjerdi, A.A., Vinagre, B.M., Chen, Y.Q., HosseinNia, S.H.: Linear fractional order controllers; a survey in the frequency domain. Annu. Rev. Control. **47**, 51–70 (2019)

26. Dawood, F.S., Iuliano, A.D., Reed, C., et al.: Estimated global mortality associated with the first 12 months of 2009 pandemic influenza A H1N1 virus circulation: a modelling study. Lancet Infect Dis. **12**, 687–695 (2012). https://doi.org/10.1016/S1473-3099(12)70121-4.PMID22738893

27. Diethelm, K., Ford, N.J., Freed, A.D.: A predictor-corrector approach for the numerical solution of fractional differential equations. Nonlinear Dyn. **29**, 3–22 (2002)

28. Duarte, J., Januario, C., Martins, N., Rogovchenko, S., Rogovchenko, Y.: Chaos analysis and explicit series solutions to the seasonally forced SIR epidemic model. J. Math. Biol. **78**, 2235–2258 (2019)

29. Duncan, S.R., Scott, S., Duncan, C.J.: Modelling the different smallpox epidemics in England. Philos. Trans. R. Soc. B (1994). https://doi.org/10.1098/rstb.1994.0158

30. El-dib, Y.O., Elgazery, N.S.: Effect of fractional derivative properties on the periodic solution of the nonlinear oscillations. Fractals **28**, 2050095 (2020)

31. Fernandes, T.S.: Chaotic model for COVID-19 growth factor. Res. Biomed. Eng. (2020). https://doi.org/10.1007/s42600-020-00077-5

32. Ge, F., Chen, Y.Q.: Optimal vaccination and treatment policies for regional approximate controllability of the time-fractional reaction–diffusion SIR epidemic systems. ISA Trans. **115**, 143–152 (2021)

33. He, S., Banerjee, S.: Epidemic outbreaks and its control using a fractional order model with seasonality and stochastic infection. Physica A **501**, 408–417 (2018)

34. Hu, Z., Teng, Z., Zhang, L.: Stability and bifurcation analysis in a discrete SIR epidemic model. Math. Comput. Simul. **97**, 80–93 (2014)

35. Huremovic, D.: Brief history of pandemics (pandemics throughout history). In: Psychiatry of Pandemics. Springer, Berlin (2019). https://doi.org/10.1007/978-3-030-15346-5_2

36. Itik, M., Banks, S.: Chaos in a three-dimensional cancer model. Int. J. Bifur. Chaos **20**, 71–79 (2010)

37. Jan, R., Khan, M.A., Kumam, P., Thounthong, P.: Modeling the transmission of dengue infection through fractional derivatives. Chaos Solitons Fractals **127**, 189–216 (2019)

38. John Hopkins University and Medicine, Coronavirus Research Centre, https://coronavirus.jhu.edu/region/india

39. Jones, A., Stigul, N.: Is spread of COVID-19 a chaotic epidemic? Chaos Solitons Fractals **181**, 138–149 (2021)

40. Kar, T.K., Mondal, P.K.: Global dynamics and bifurcation in delayed SIR epidemic model. Nonlinear Anal. Real World Appl. **12**, 2058–2068 (2011)

41. Karbasizadeh, N., Saikumar, N., HosseinNia, S.H.: Fractional-order single state reset element. Nonlinear Dyn. **104**, 413–427 (2021). https://doi.org/10.1007/s11071-020-06138-9

42. Khanjanchi, S., Perc, M., Ghosh, D.: The influence of time delay in a chaotic cancer model. Chaos **28**, 103101 (2018)

43. Khanna, R.C., Cicinelli, M.V., Gilbert, S.S., Honavar, S.G., Murthy, G.V.S.: COVID-19 pandemic: lessons learned and future directions. Indian J. Ophthalmol. **68**, 703–710 (2020)

44. Kooi, B.W., Aguiar, M., Stollenwerk, N.: Bifurcation analysis of a family of multi-strain epidemiology models. J. Comput. Appl. Math. **252**, 148–158 (2013)

45. Li, L., Sun, G.Q., Jin, Z.: Bifurcations and chaos in an epidemic model with nonlinear incidence rates. Appl. Math. Comput. **216**, 1226–1234 (2010)

46. Li, Q., Xiao, Y.: Dynamic behaviour and bifurcation analysis of the SIR model with continuous treatment and state-dependent impulsive control. Int. J. Bifur. Chaos **29**, 1950131 (2019)

47. Li, T., Wang, Y., Zhao, C.: Synchronization of fractional chaotic systems based on a simple Lyapunov function. Adv. Differ. Equ. (2017). https://doi.org/10.1186/s13662-017-1320-1

48. Lin, T., Lee, T., Balas, V.E.: Adaptive fuzzy sliding mode control for synchronisation of uncertain fractional order chaotic systems. Chaos Solitons Fractals **44**, 791–801 (2011)

49. Lu, Z., Yu, Y., Chen, Y., Ren, G., Xu, C., Wang, S., Yin, Z.: A fractional-order SEIHDR model for COVID-19 with inter-city networked coupling effects. Nonlinear Dyn. **101**, 1717–1730 (2020)

50. Luo, Y., Zhang, T., Lee, B., Kang, C., Chen, Y.: Fractional-order proportional derivative controller synthesis and implementation for hard-disk-drive servo system. IEEE Trans. Control Syst. Technol. **22**, 281–289 (2014)

51. Mangiarotti, S.: Low dimensional chaotic models for the plague epidemic in Bombay (1896–1911). Chaos Solitons Fractals **81**, 184–196 (2015)

52. Mangiarotti, S., Peyre, M., Huc, M.: A chaotic model for the epidemic of Ebola virus disease in West Africa (2013–2016). Chaos **26**, 113112 (2016)

53. Mangiarotti, S., Peyre, M., Zhang, Y., Huc, M., Roger, F., Kerr, Y.: Chaos theory applied to the outbreak of COVID-19: an ancillary approach to decision making in pandemic context. Epidemiol. Infect. **148**, 1–9 (2020). https://doi.org/10.1017/S0950268820000990

54. Maira, A., Kooi, B., Stollenwerk, N.: Epidemiology of dengue fever: a model with temporary cross-immunity and possible secondary infection shows bifurcations and chaotic behaviour in wide parameter regions. Math. Model. Nat. Phenom. **3**, 48–70 (2008)

55. Marur, S., D'Souza, G., Westra, H.W., Forastiere, A.A.: HPV-associated head and neck cancer: a virus-related cancer epidemic. Lancet Oncol. **11**, 781–789 (2010)

56. McLennan-Smith, T.A., Geoffry, N.M.: Complex behaviour in a dengue model with a seasonally varying vector population. Math. Biosci. **248**, 22–30 (2014)

57. Nazarimehr, F., Jafari, S., Hashemi Golpayegani, S.M.R., et al.: Can Lyapunov exponent predict critical transitions in biological systems? Nonlinear Dyn. **88**, 1493–1500 (2017). https://doi.org/10.1007/s11071-016-3325-9

58. Nowzari, C., Preciado, V.M., Pappas, G.J.: Analysis and control of epidemics: a survey of spreading processes on complex networks. IEEE Control Syst. Mag. **36**, 26–46 (2016)

59. Ong, A., Sandar, M., Chen, M.I., Sin, L.Y.: Fatal dengue hemorrhagic fever in adults during a dengue epidemic in Singapore. Int. J. Infect. Dis. **11**, 263–267 (2007)

60. Pedro, S.A., Abelman, S., Ndjomatchoua, F.T., Sang, R., Tonnang, H.E.Z.: Stability, bifurcation and chaos analysis of vector-borne disease model with application to rift valley fever. PLoS ONE (2014). https://doi.org/10.1371/journal.pone.0108172

61. Plague Research Commission: The epidemiological observations made by the commissioning Bombay city. J. Hyg. **7**, 724–798 (1907)

62. Pollitzer, R.: Plague, pp. 409–482. WHO, Geneva (1954)

63. Proctor, R.N.: Tobacco and the global lung cancer epidemic. Nat. Rev. Cancer **1**, 82–86 (2001). https://doi.org/10.1038/35094091

64. Qian, L., Yanni, X.: Dynamical behaviour and bifurcation analysis of the SIR model with continuous treatment and state-dependent impulsive control. Int. J. Bifurc. Chaos **29**, 10 (2019). https://doi.org/10.1142/S0218127419501311

65. Rajagopal, K., Akgul, A., Jafari, S., et al.: A chaotic memcapacitor oscillator with two unstable equilibriums and its fractional form with engineering applications. Nonlinear Dyn. **91**, 957–974 (2017). https://doi.org/10.1007/s11071-017-3921-3

66. Rajagopal, K., Hasanzadeh, N., Parastesh, F., et al.: A fractional-order model for the novel coronavirus (COVID-19) outbreak. Nonlinear Dyn. **101**, 711–718 (2020). https://doi.org/10.1007/s11071-020-05757-6

67. Rihan, F.A., Al Mdallal, Q.M., AlSakaji, H.J., Hashish, A.: A fractional-order epidemic model with time-delay and nonlinear incidence rate. Chaos Solitons Fractals **126**, 97–105 (2019)

68. Righetto, L., Casagrandi, R., Bertuzzo, E., Mari, L., Gatto, M., Rodriguez-Iturbe, I., Rinaldo, A.: The role of aquatic reservoir fluctuations in long-term cholera patterns. Epidemics **4**, 33–42 (2012)

69. Roopaei, M., Sahraei, B.R., Lin, T.C.: Adaptive sliding mode control in a novel class of chaotic systems. Commun. Nonlinear Sci. Numer. Simul. **15**, 4158–4170 (2010)

70. Seward, J.F., Galil, K., Damon, I., Norton, S.A., Rotz, L., Schmid, S., Harpaz, R., Cono, J., Marin, M., Hutchins, S., Chaves, S.S., McCauley, M.M.: Development and experience with an algorithm to evaluate suspected smallpox cases in the United States, 2002–2004. Clin. Infect. Dis. **39**, 1477–1483 (2004)

71. Shaikh, A.S., Nisar, K.S.: Transmission dynamics of fractional order typhoid fever model using Caputo–Fabrizio operator. Chaos Solitons Fractals **128**, 355–365 (2019)

72. Speakman, M., Sharpley, R.: A chaos theory perspective on destination crisis management: Evidence from Mexico. J. Destin. Mark. Manag. **1**, 67–77 (2012)

73. Subchan, F.I., Syaf, A.M.: An epidemic cholera model with control treatment and intervention. J. Phys. Conf. Ser. **1218**, 012046 (2019)

74. Tan, W., Gao, J., Fang, W.: Bifurcation analysis and chaos control in a discrete epidemic system. Discret. Dyn. Nat. Soc. (2015). https://doi.org/10.1155/2015/974868

75. Takagi, T., Sugeno, M.: Fuzzy identification of systems and its applications to modeling and control. IEEE Trans. Syst. Man. Cyber. **15**, 116–132 (1985)

76. Tene, A.G., Tchoffo, M., Tabi, B.C., Kofane, T.C.: Generalized synchronization of regulate seizures dynamics in partial epilepsy with fractional-order derivatives. Chaos Solitons Fractals. **132**, 109553 (2020)

77. Trifonov, V., Khiabanian, H., Rabadan, R.: Geographic dependence, surveillance, and origins of the 2009 influenza A (H1N1)virus. N. Engl. J. Med. **361**, 115–119 (2009). https://doi.org/10.1056/NEJMp0904572.PMID19474418

78. Upadhyay, R.K., Roy, P.: Deciphering dynamics of recent epidemic spread and outbreak in West Africa: the case of Ebola virus. Int. J. Bifurc. Chaos **26**, 1630023 (2016). https://doi.org/10.1142/S021812741630024X

79. Upadhyay, R.K., Roy, P., Rai, V.: Deciphering dynamics of epidemic spread: the case of influenza virus. Int. J. Bifurc. Chaos **24**, 1450064 (2014). https://doi.org/10.1142/S0218127414500643

80. Vaidyanathan, S.: Takagi-Sugeno fuzzy logic controller for Liu-Chen four-scroll chaotic system. Intell. Engi. Inf. **4**, 135–150 (2016)

81. Valle, P.A., Coria, L.N., Gamboa, D., Plata, C.: Bounding the dynamics of a chaotic-cancer mathematical model. Hindawi Math. Prob. Eng. (2018). https://doi.org/10.1155/2018/9787015

82. Volos, C., Akgul, A., Pham, V.T., et al.: A simple chaotic circuit with a hyperbolic sine function and its use in a sound encryption scheme. Nonlinear Dyn. **89**, 1047–1061 (2017). https://doi.org/10.1007/s11071-017-3499-9

83. Yi, N., Zhang, Q., Mao, K., Yang, D., Li, Q.: Analysis and control of an SEIR epidemic system with nonlinear transmission rate. Math. Comput. Model. **50**, 1498–1513 (2009)

84. Yi, N., Zhang, Q., Liu, P., Lin, Y.: Codimension-two bifurcations analysis and tracking control on a discrete epidemic model. J. Syst. Sci. Complex **24**, 1033–1056 (2011)

85. Zhang, Y., Zhang, Q.L., Zhang, F.: Chaos analysis and control for a class of SIR epidemic model with seasonal fluctuation. Int. J. Biomath. **6**, 1250063 (2013). https://doi.org/10.1142/S1793524512500635

86. Zhang, Q., Tang, B., Tang, S.: Vaccination threshold size and backward bifurcation of SIR model with state-dependent pulse control. J. Theor. Biol. **455**, 75–85 (2018)